Simulations of Photonic Crystal and Dielectric Structures

Greg Werner

Contributors: Sergey Antipov, Carl Bauer, Alan Cook, Ben Cowan, Chunguang Jing, Chris McGuinness, Peter Messmer, Brian Munroe, Gennadij V. Sotnikov

Outline

- Codes and algorithms for full-wave simulation of dielectrics
  - Finite Difference/Finite Integration
  - FEM
  - Nonlinear/dispersive dielectrics
- Dielectric structures
  - Dielectric Loaded (cylindrical) Accelerator structures
  - DLA power extractor
  - 2-channel DLA wakefield accelerator
- Photonic crystal structures
  - MAP structures
  - Photonic quasi-crystals
  - Optimization away from lattice
  - Overmoded, modified lattice
  - Woodpile
- Nonlinear/dispersive dielectrics and metamaterials
- Faster computation with GPUs?

Simulation and Approximation

Oversimplification: Simulation is basically truncated Taylor expansion
(or expansion in basis of choice: polynomial, Fourier, ...)

$$f'(x) = \frac{f(x+\Delta x) - f(x)}{\Delta x} + O(\Delta x/\lambda)$$

First order error.

$$f'(x) = \frac{f(x+\Delta x/2) - f(x-\Delta x/2)}{\Delta x} + O(\Delta x/\lambda)^2$$

Second order error.

scale over which f varies

If only it were this easy....

Accuracy as $\Delta x/\lambda \rightarrow 0$ and $\Delta t/T \rightarrow 0$ is necessary, but not sufficient:

- Some behavior needs to be exact: e.g., energy conservation, charge conservation.
- There are modes for which $\Delta x/\lambda$ or $\Delta t/T$ are not close to zero.

Example of accurate but (probably) not useful

$$f'(x) = \frac{f(x+\Delta x) - f(x-\Delta x)}{2\Delta x} + O(\Delta x/\lambda)^2$$ has second order error, but:

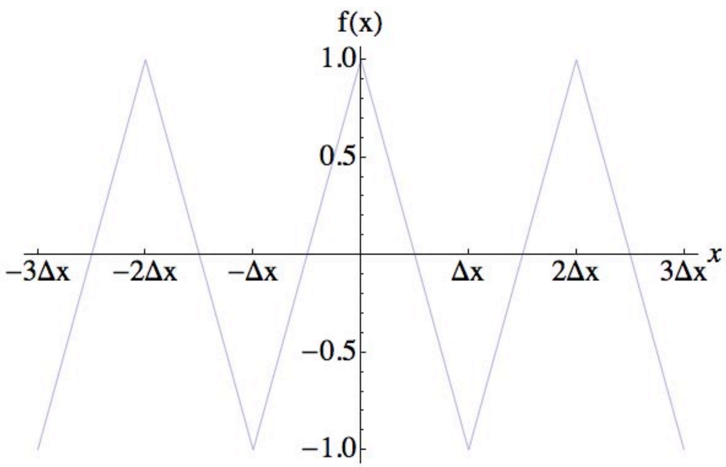

yields $f'(0) \approx 0$

This could cause a very short-wavelength mode to have a very low frequency.

Convergence of algorithms for Cartesian mesh

2D PhC square lattice of isotropic dielectric cylinders in vacuum

MITPhotonicBands

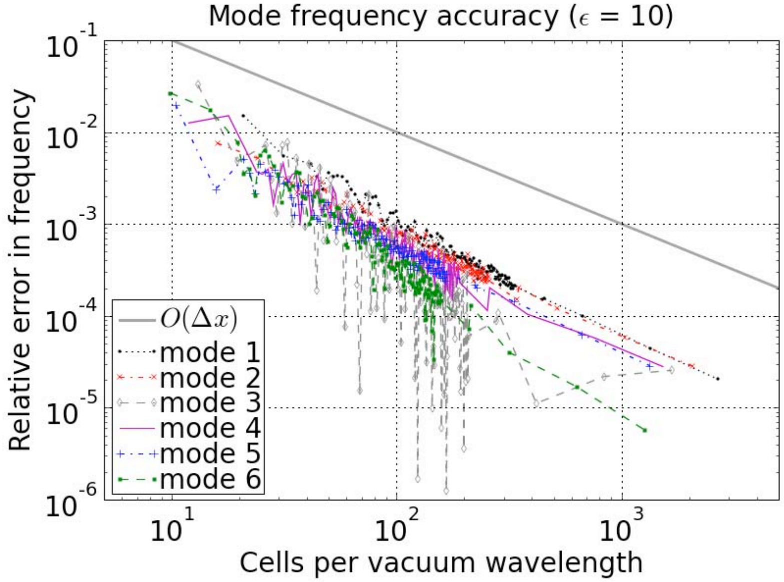

VORPAL-effective dielectric (for low contrast)

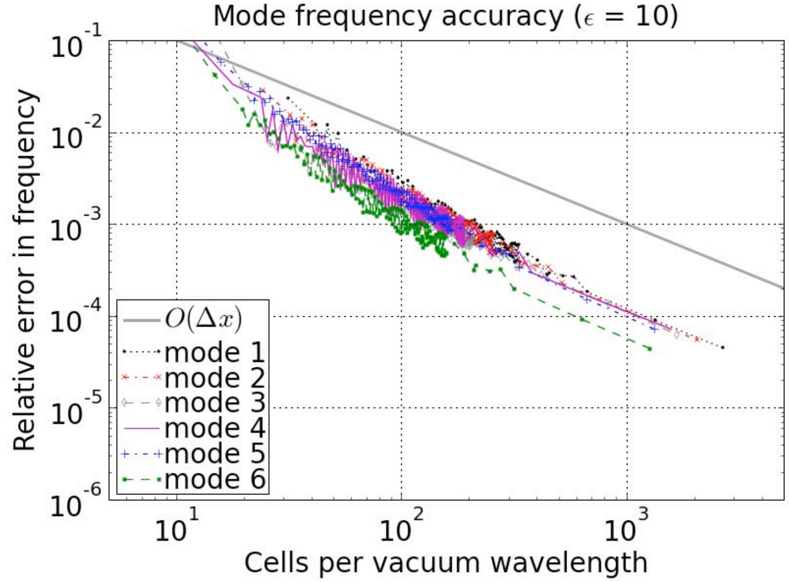

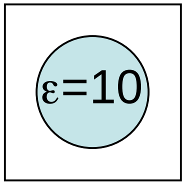

stairstep

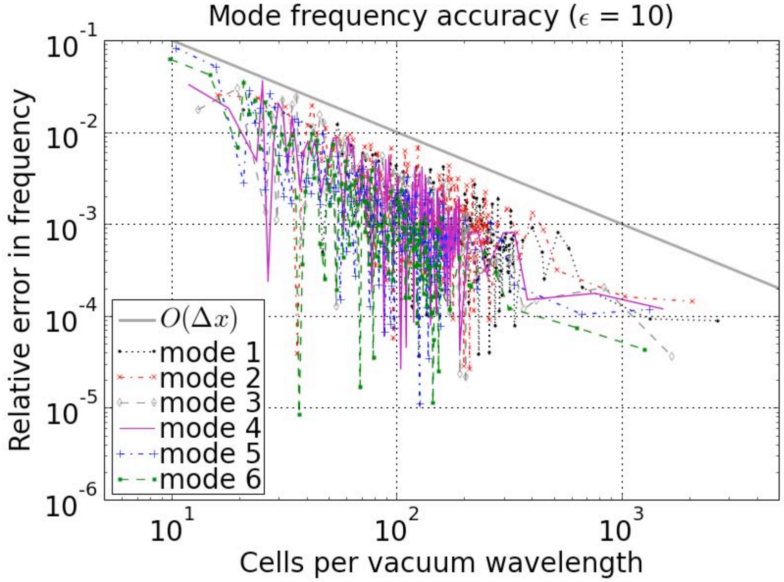

VORPAL-effective dielectric (for high contrast)

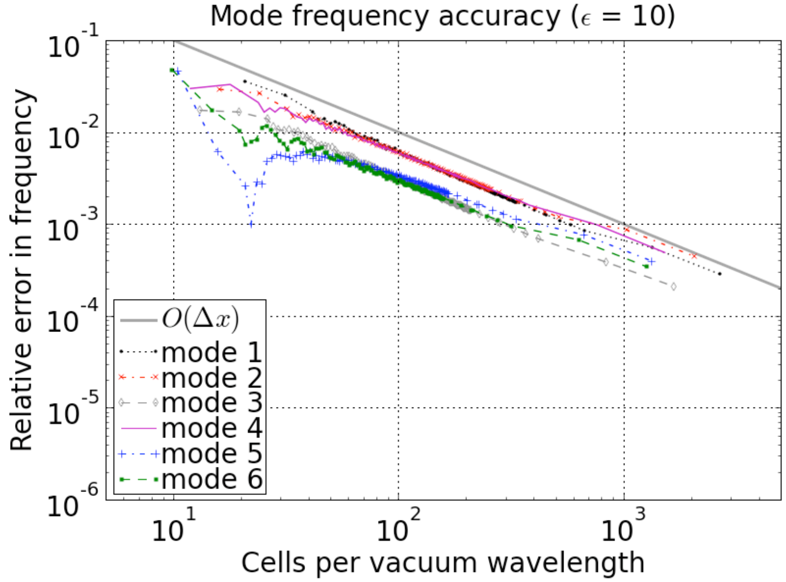

Convergence of algorithms for Cartesian mesh

2D PhC square lattice of isotropic dielectric cylinders in vacuum

MitPhotonicBands

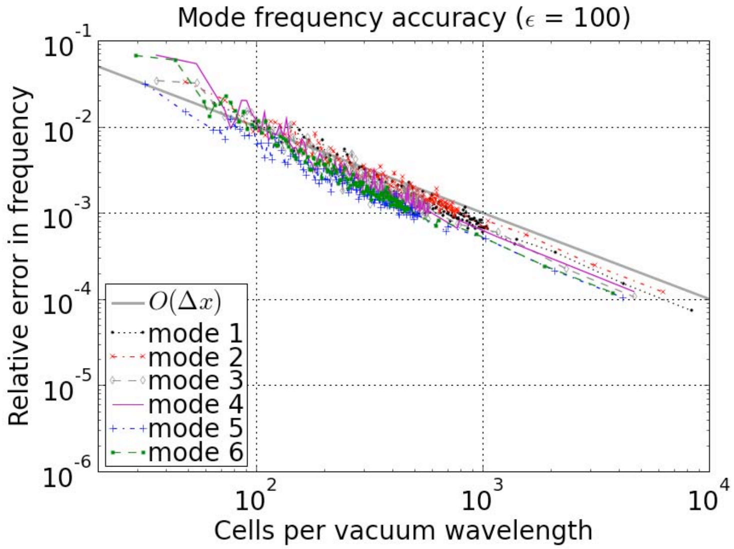

VORPAL-effective dielectric (for low contrast)

This algorithm is unstable for (approx.) ε>20, though it can be smoothly mixed with algorithm below to achieve better stability and accuracy.

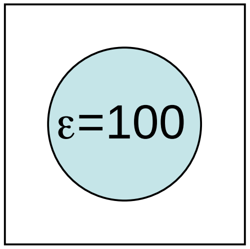

stairstep

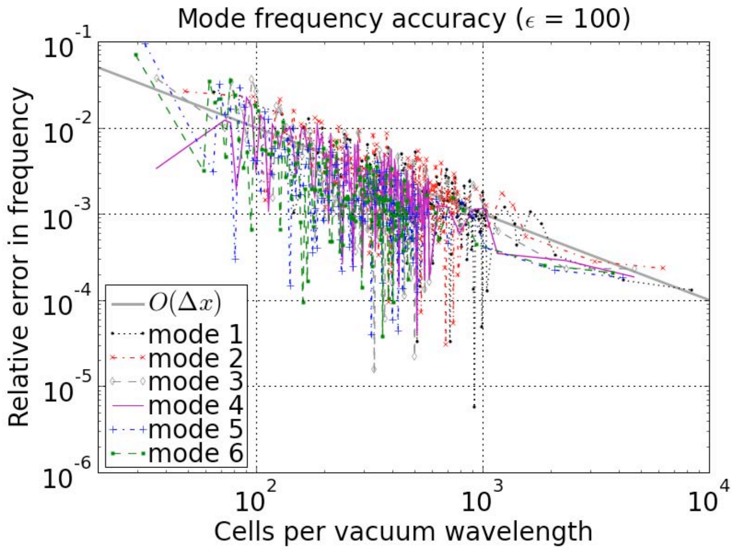

VORPAL-effective dielectric (for high contrast)

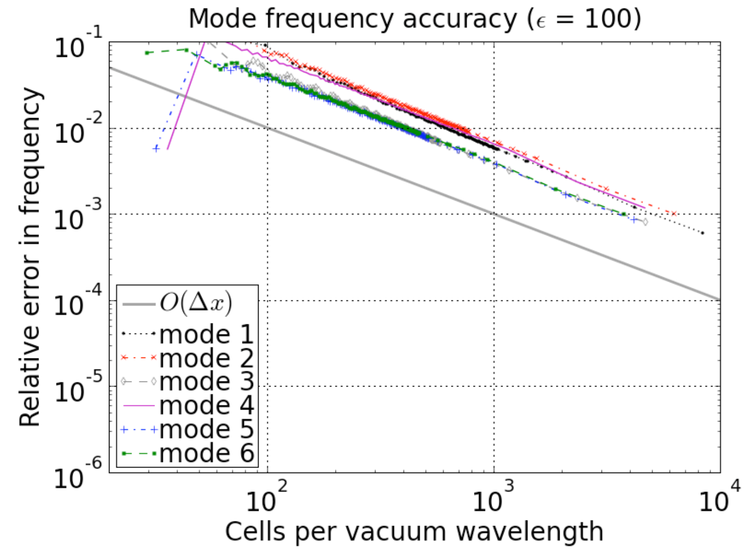

Finite Difference with O(Δx²) error

ε=10

Isotropic dielectric sphere, inside metal sphere, compared against exact solution, shows 2nd order error in resonant frequencies.

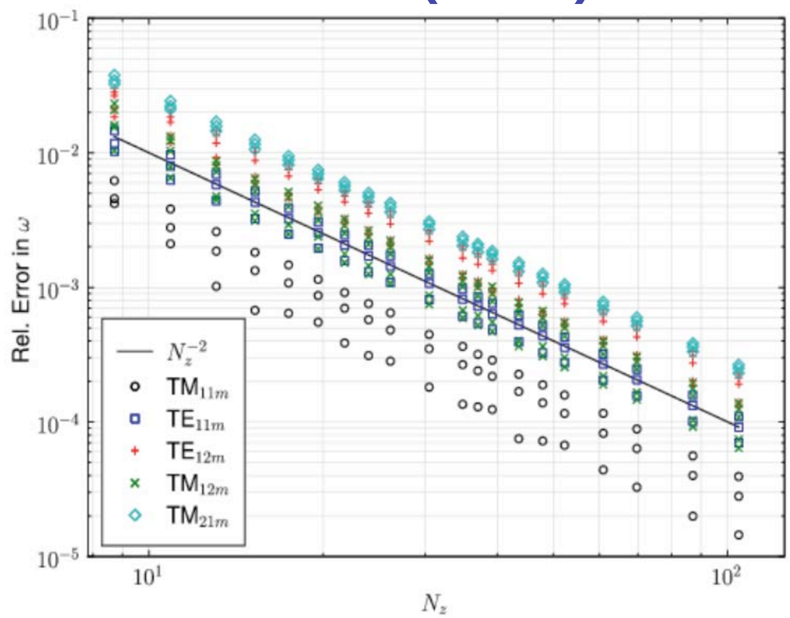

Unfortunately, this algorithm is unstable in the time domain.

- Cubic lattice of rotated dielectric ellipsoids.
- Comparison with Richardson extrapolation from 96^3 and 128^3

$$\varepsilon = \mathbf{R}^{\mathrm{T}} \begin{bmatrix} 8 & & \\ & 10 & \\ & & 12 \end{bmatrix} \mathbf{R}$$

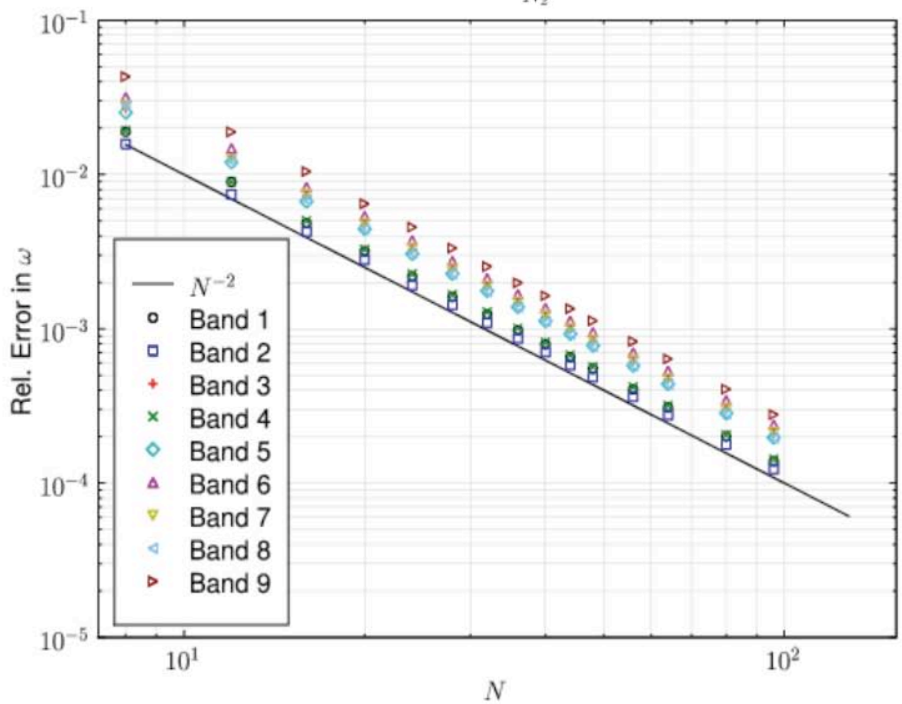

See talk by Carl Bauer, WG2/3 Thurs Afternoon.

Fields also have O(Δx^2) error even near boundary

- Dielectric cylinder (ε = 10) inside metal cylinder
- 2D TE quarter simulation to eliminate degeneracies
- Azimuthal ring of 100 sample points 5 cells from boundary in vacuum (sample points get closer to boundary as resolution increases)

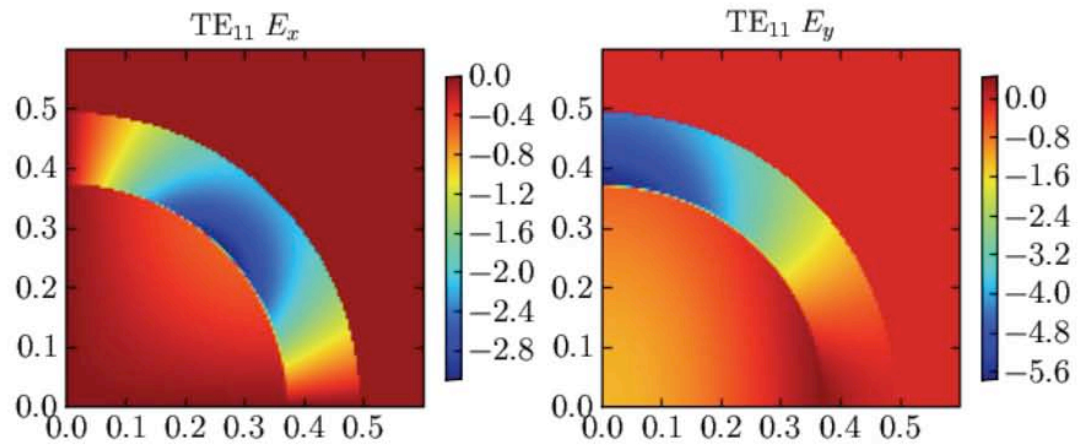

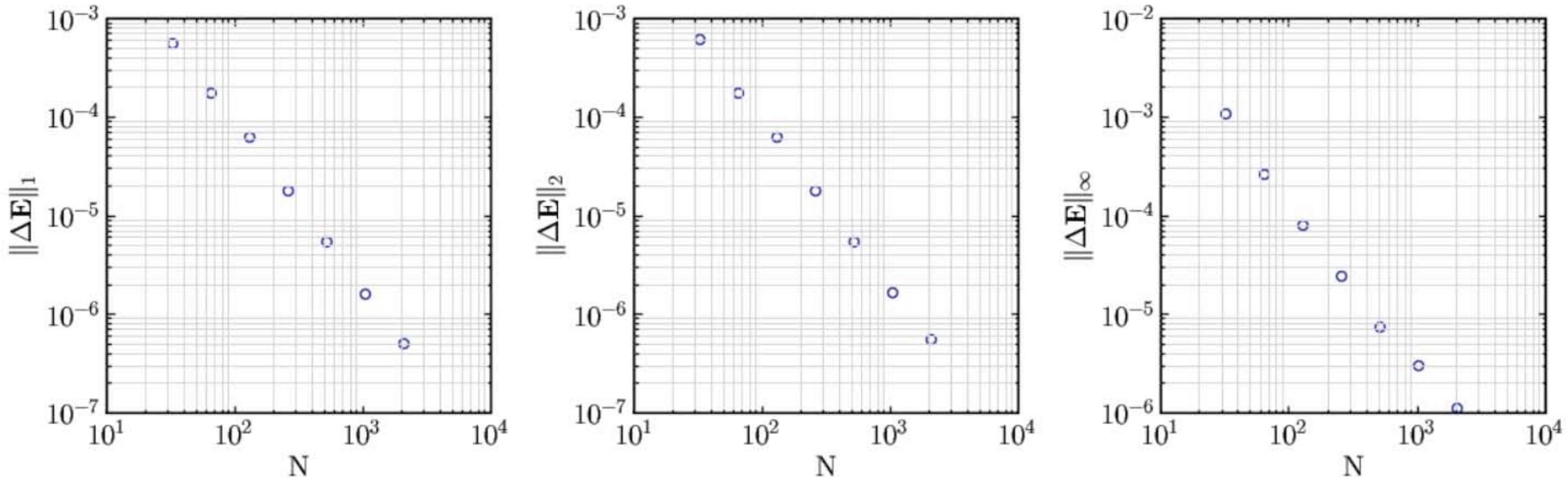

See AAC talk by Carl Bauer, WG2/3 Thurs Afternoon.

Finite Element Method

By using meshes that conform to the surfaces of the simulated objects, and by using high-order basis elements, FEM can simulate complicated shapes with high accuracy. Furthermore, localized mesh refinement can be used to simulate small features accurately.

See AAC presentations by SLAC Advanced Computations Dept.
Cho Ng (WG2 Tues. late afternoon)
Arno Candel, Cho Ng (WG2/3 Thurs. late afternoon)

Kinds of dielectrics to simulate

- Isotropic
- Anisotropic
- Lossy
- Nonlinear
- Dispersive

Dielectric Loaded Accelerator structure

DLA structure based on the coaxial coupler design

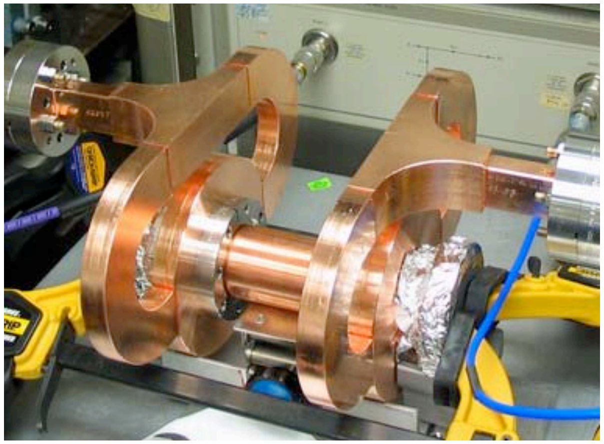

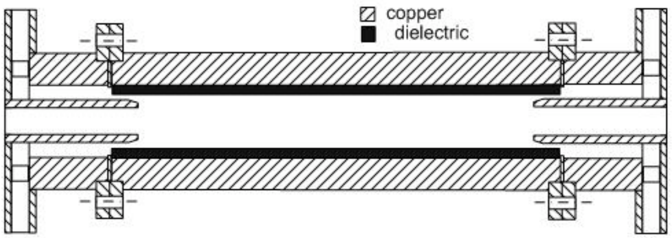

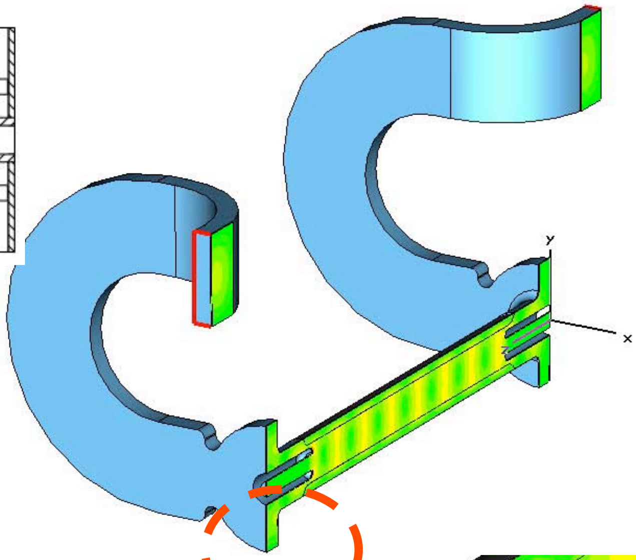

Simulated by CST Microwave Studio

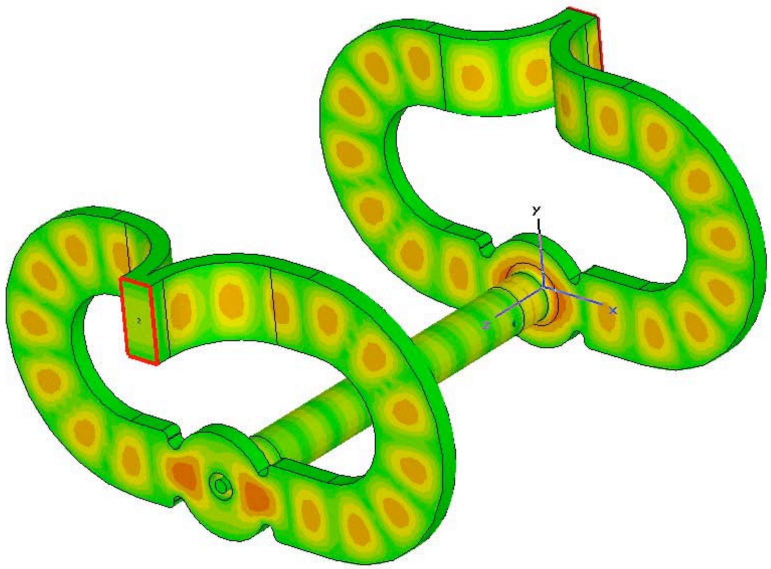

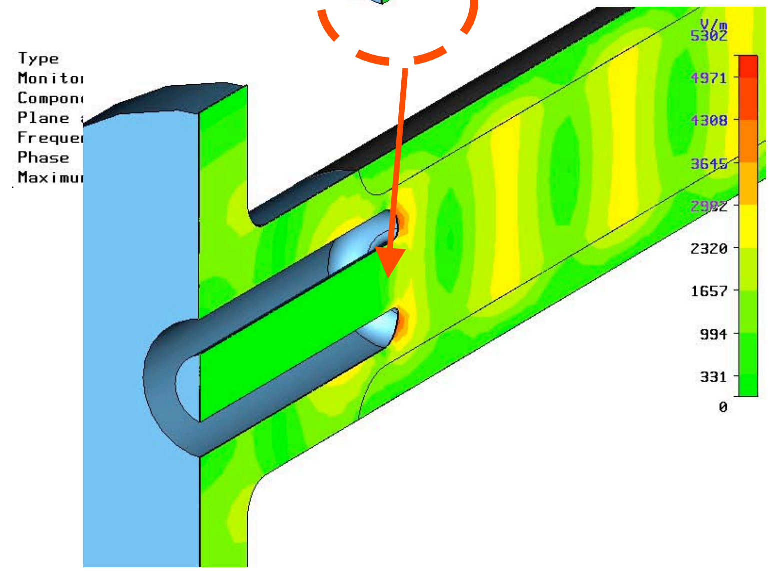

Type = E-Field (peak)
Monitor = e-field (f=11.424) [1]
Component = Abs
Maximum-3d = 5847.91 V/m at 3 / 0 / 21.37
Frequency = 11.424
Phase = 0 degrees

See AAC talks by

S. Antipov (WG3 Wed afternoon)

C. Jing (WG3 Thurs morning)

euclid TECHLABS

Argonne NATIONAL LABORATORY

Dielectric Loaded Accelerator structure

Multi-layer DLA structure: reduce H, hence current, at outer metal surface to reduce losses. Operating in TM03 mode reduces losses by a factor of 6 with comparable shunt impedance (compared to single layer structure in TM01 mode)

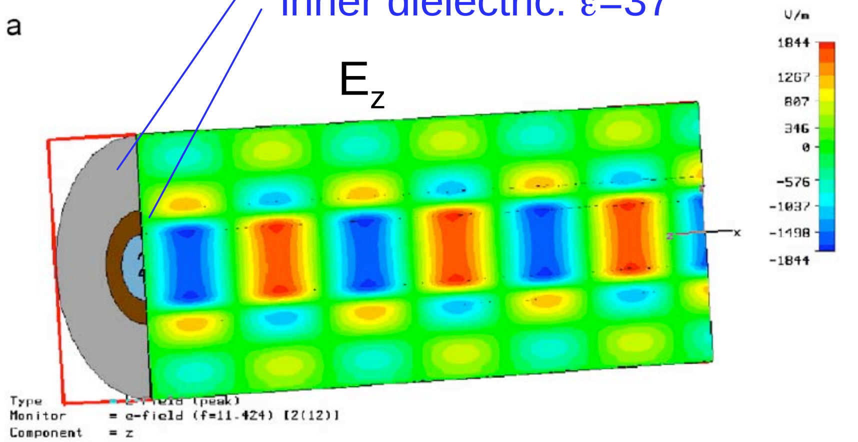

Simulations with CST Microwave Studio

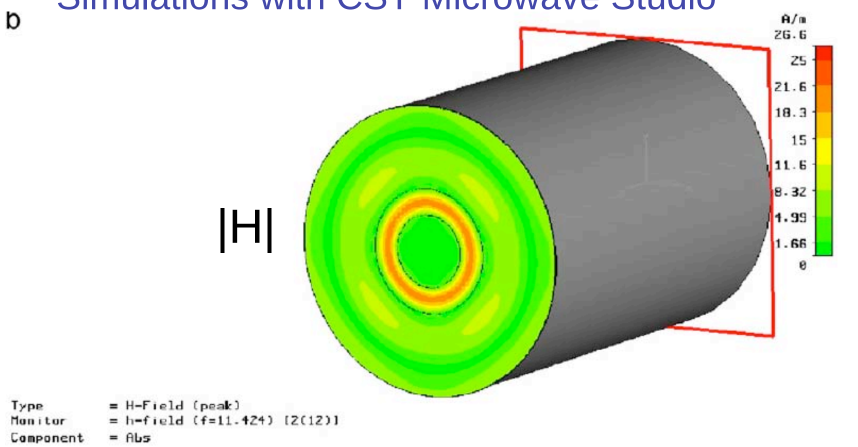

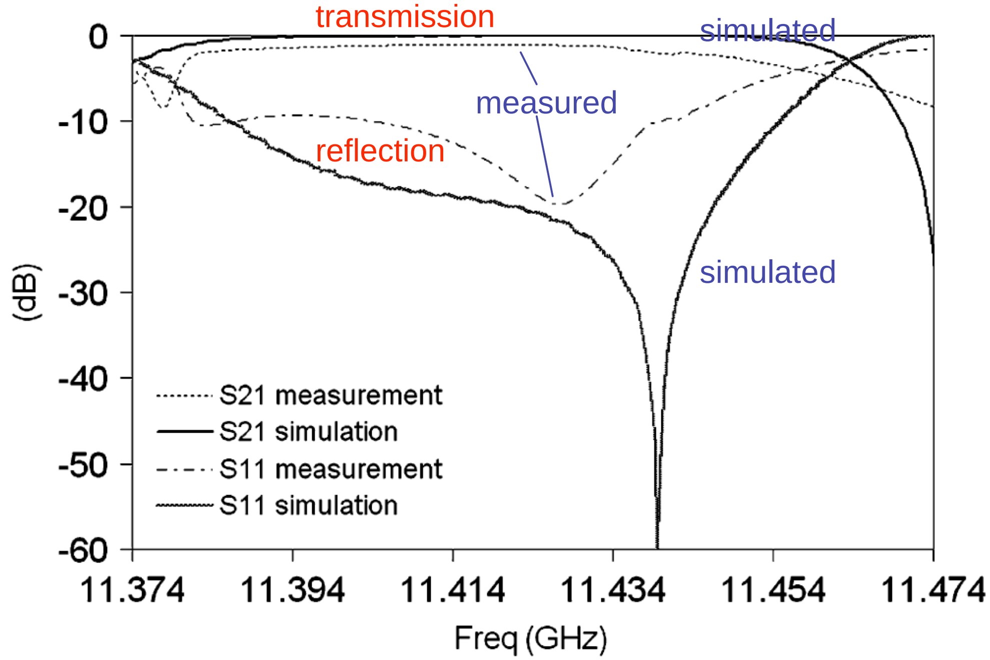

Differences due to losses (neglected in simulation), and small mismatches in VNA-DLA mode converter.

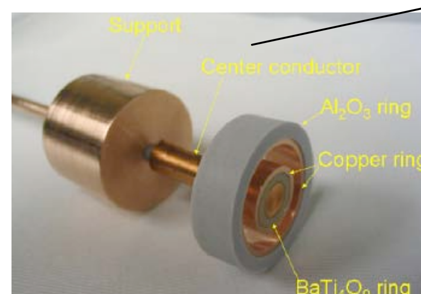

See C. Jing et. al., NIM A 594, 132 (2008)
and AAC talks: WG3 Wed and Thurs mornings

euclid TECHLABS
Argonne NATIONAL LABORATORY

Power extraction from dielectric loaded WG

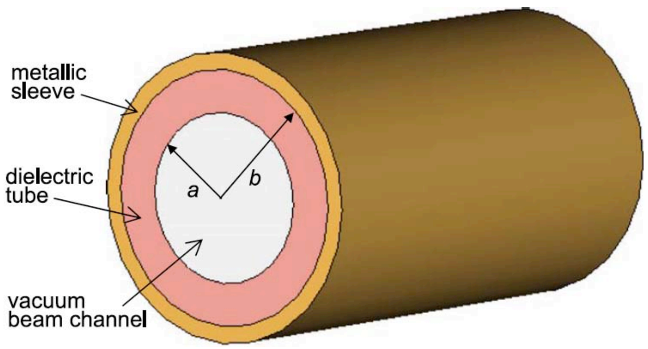

Simulation done by CST Microwave Studio.

7.8GHz Dielectric-Based Wakefield Power Extractor

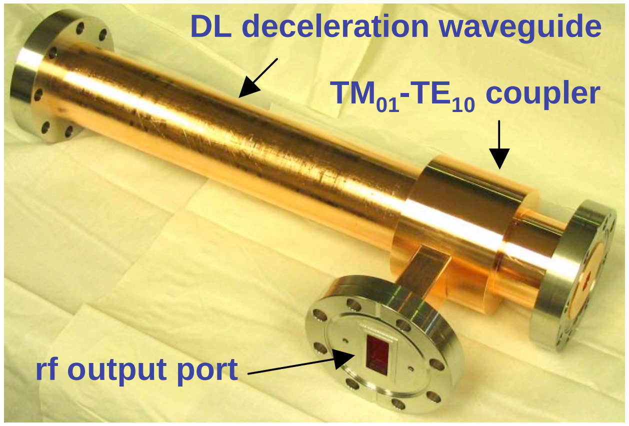

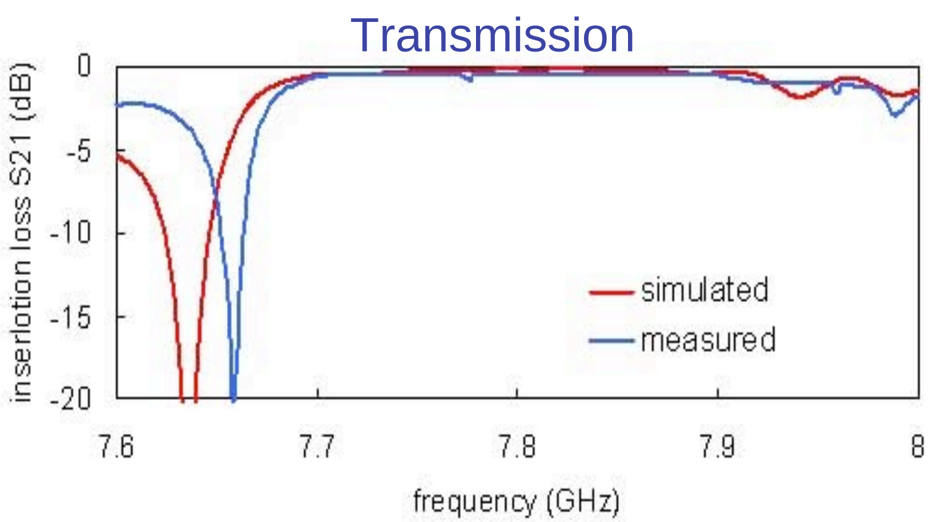

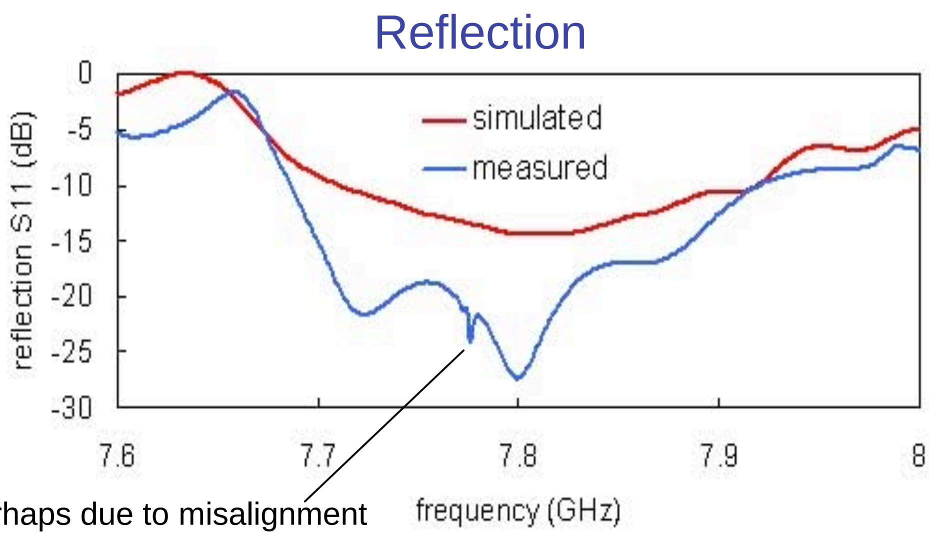

perhaps due to misalignment of dielectric tube

See:
F. Gao et. al., PRSTAB 11, 041301 (2008)
F. Gao et. al., NIM A 609, 89 (2009)
C. Jing et. al., IPAC 2010, THPD067 (2010).
and AAC talks: WG3 Wed and Thurs mornings

Power extraction from dielectric loaded WG

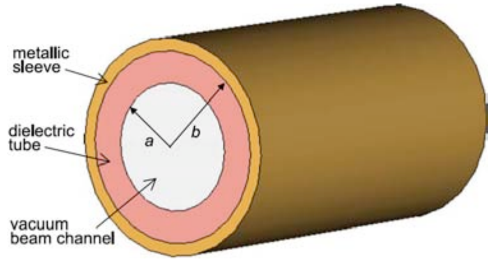

26GHz Dielectric-Based Wakefield Power Extractor----power estimation

MAFIA TS2 Wakefield simulation

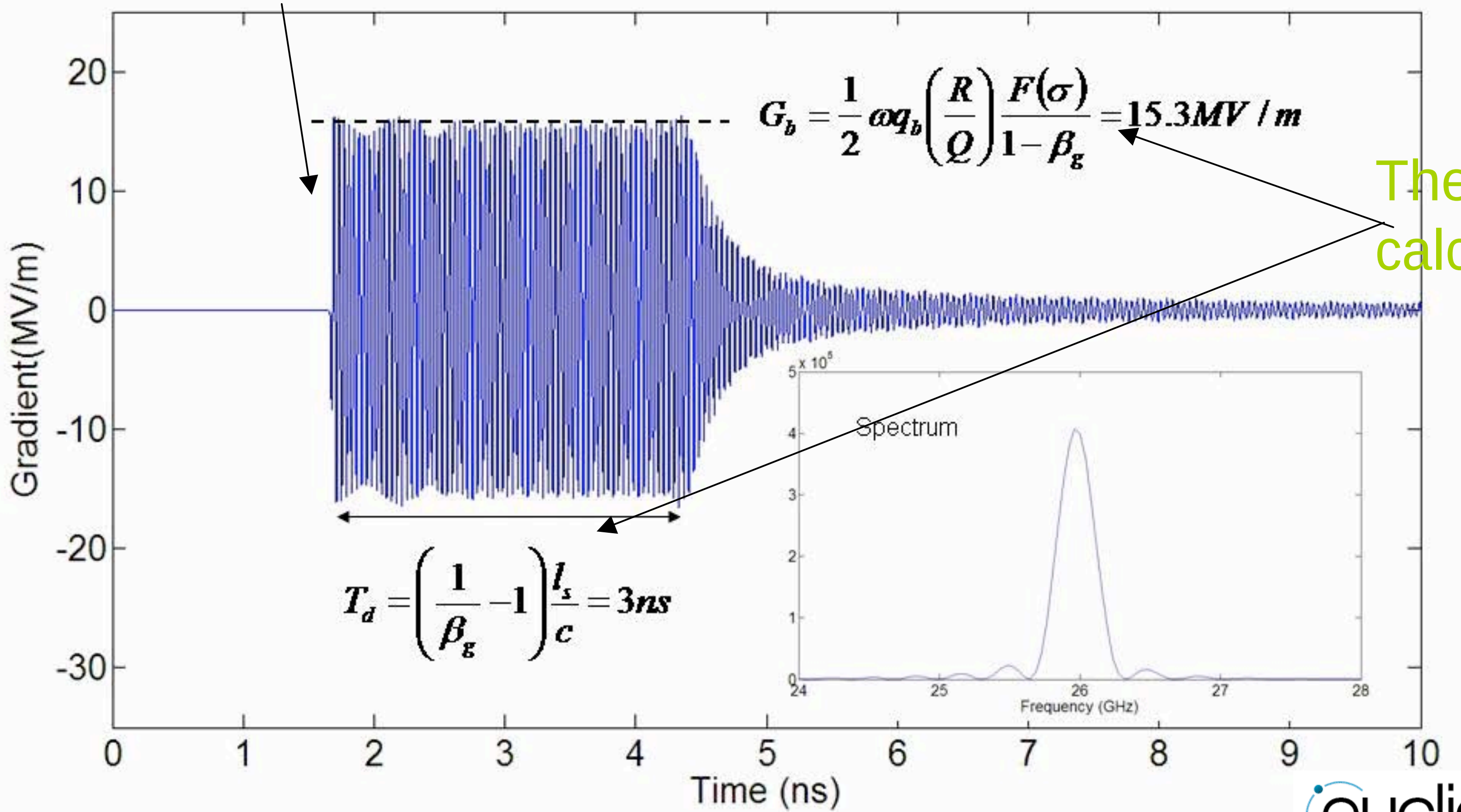

Theoretical calculation

See AAC talks by C. Jing: WG3 Wed and Thurs mornings

2-channel wakefield accelerator

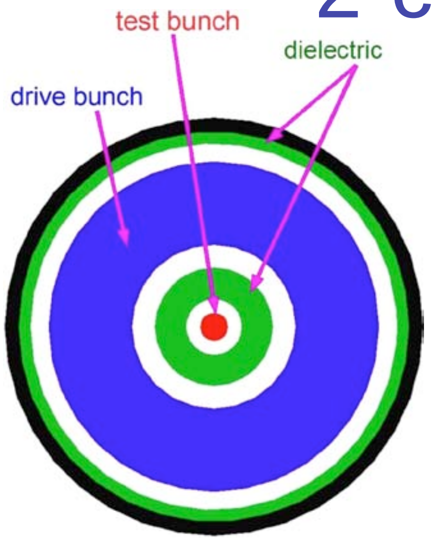

The low-energy drive bunch excites (wake)fields that accelerate a high-energy test bunch.

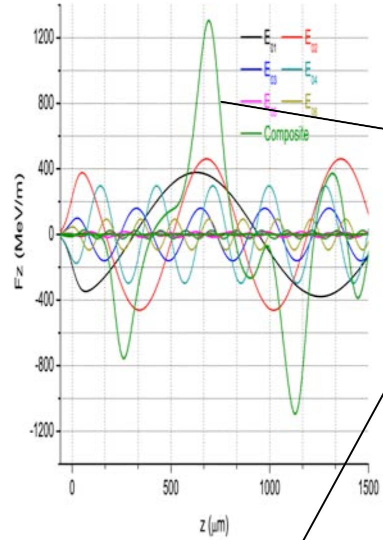

Analytic axial wakefield result, in green (for infinite tube)

Simulation in blue (conducting boundary at entry) using CST Particle Studio: 3D, 10^7 cells (variable size), 2600 time steps, 0.12 us/cell-step (Core 2 Duo).

Axial electric field behind drive bunch:
analytic theory for infinite tube predicts “periodic” wake;
simulation finds that, somewhat independent of entry boundary condition, a quenching wave damps the wakefield.

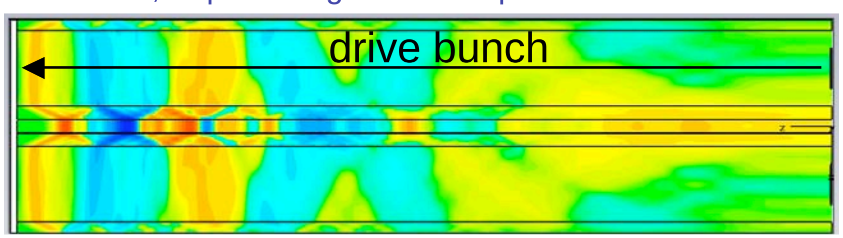

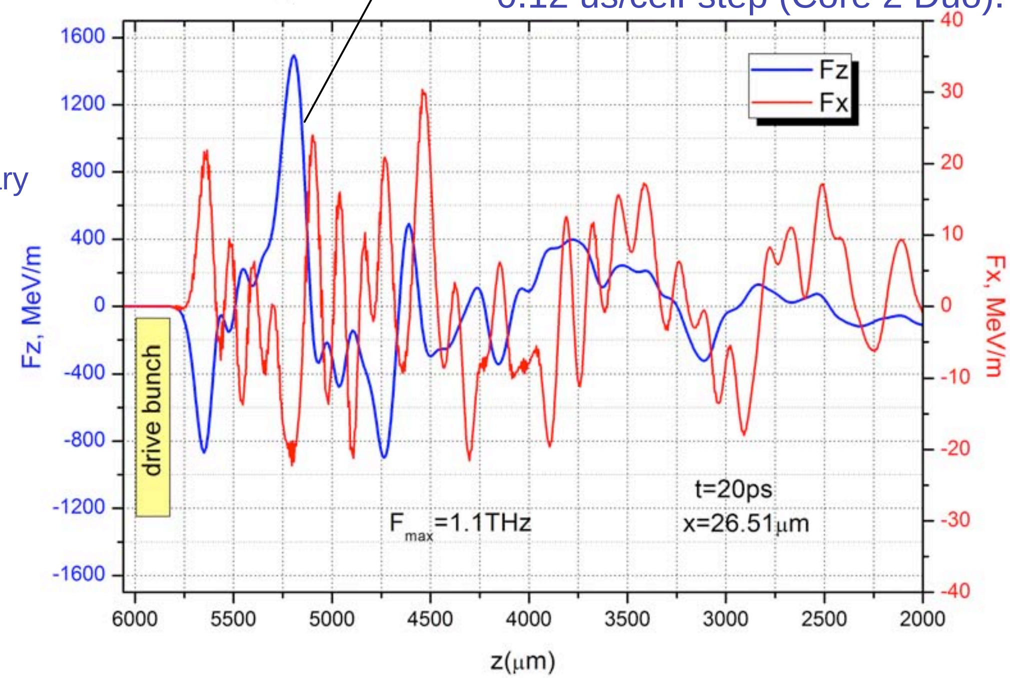

See G. V. Sotnikov, T. C. Marshall, and J. L. Hirshfield, PRSTAB 12, 061302 (2009), and AAC talks: WG3 Wed morning

Photonic Crystals (PhC)

Photonic crystals are regular lattices of dielectric or metal objects.

PhCs allow transmission of most light, but reflect frequencies that fall within a bandgap; PhCs are selective reflectors.

EM fields at frequencies within a bandgap decay exponentially as they penetrate the crystal; such fields can be localized around a defect in the lattice.

A 1D PhC
(a dielectric mirror)

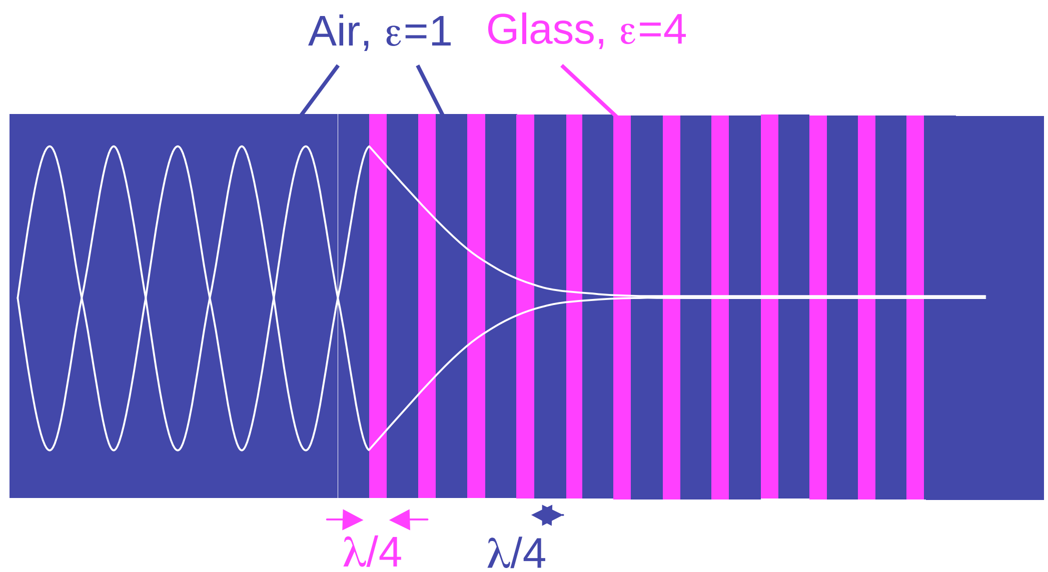

Destructive interference prevents this wavelength from propagating through the PhC; therefore, it is reflected (and fields decay exponentially into the PhC)

RF Resonant Cavities in PhCs

A defect in a triangular lattice of alumina rods (a 2D PhC) traps a resonant mode; the fields decay exponentially away from the defect. If the lattice were infinite, and the alumina lossless, the mode would be perfectly trapped (infinite Q factor).

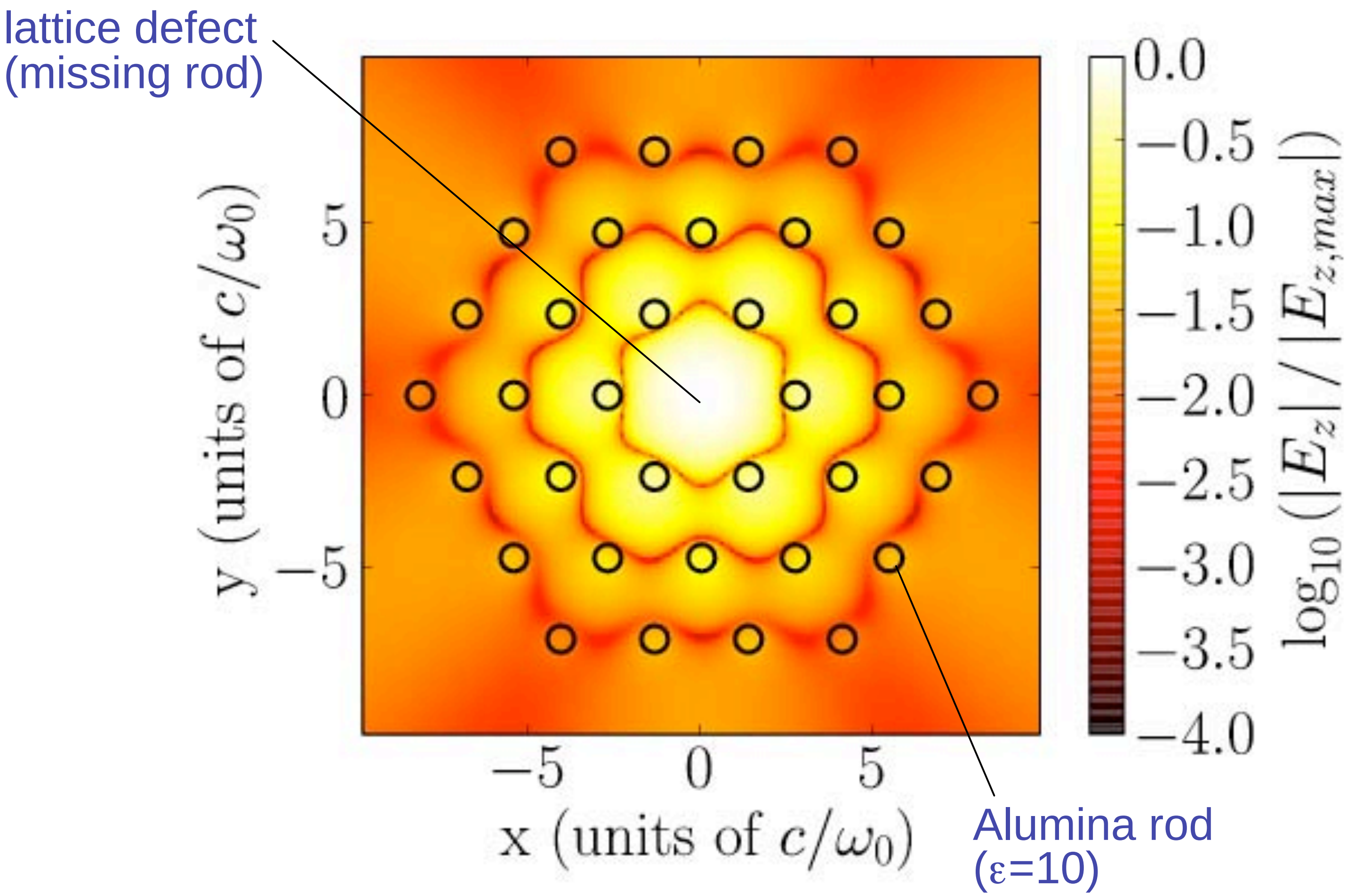

MAP structures

Micro Accelerator Platform

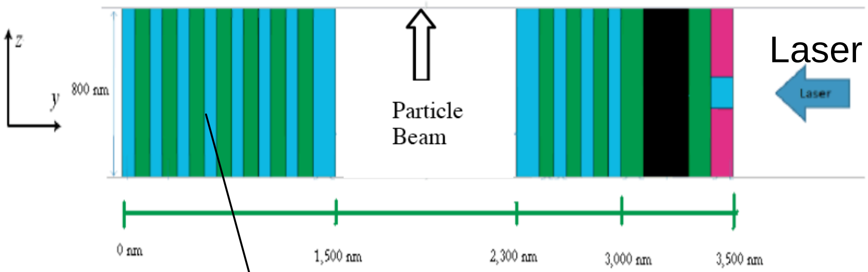

Bragg reflector (dielectric mirror, 1D PhC)

Optimizing the materials/dimensions for Bragg reflector yields better resonance:

coke-bottleing

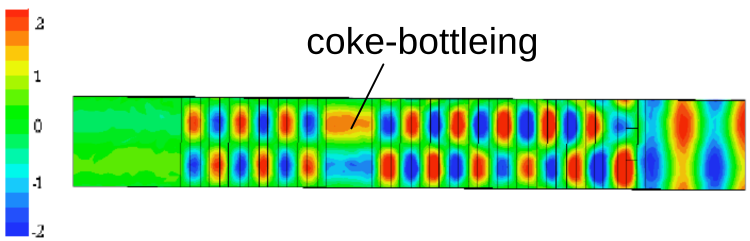

Figure 2: Color field map of E_z in the MAP exhibiting "coke-bottleing", normalized to the drive laser amplitude (color available online).

uniform fields, strong resonance

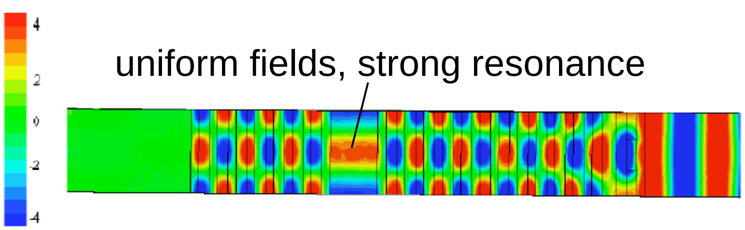

Figure 3: Color field map of E_z in the MAP exhibiting strong resonance, normalized to the drive laser amplitude.

Design for low-beta (slow) particles:

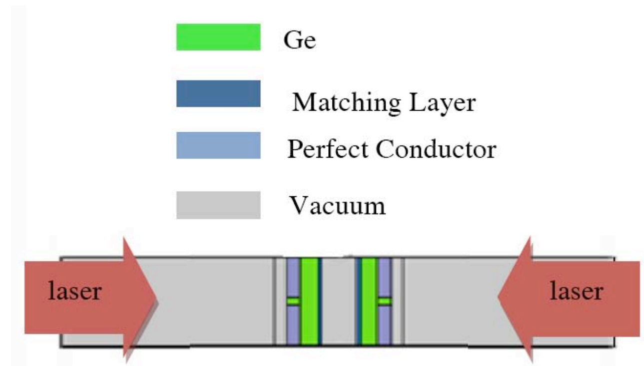

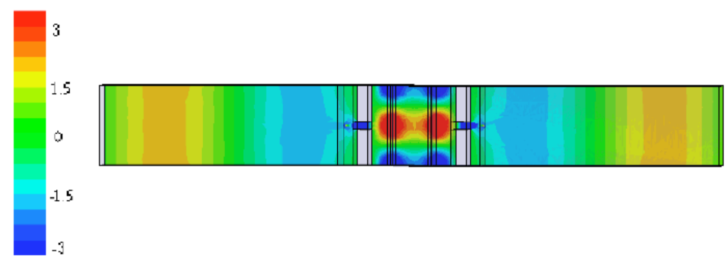

Figure 5: Resonance in low beta simplified MAP due to two incident oppositely propagating lasers, normalized to the drive laser amplitude.

See J. McNeur et. al., IPAC 2010 THPD047.
And see talk by Josh McNeur: WG3 Fri morning

TM01-like modes in QuasiCrystals

using sapphire rods with copper end-plates

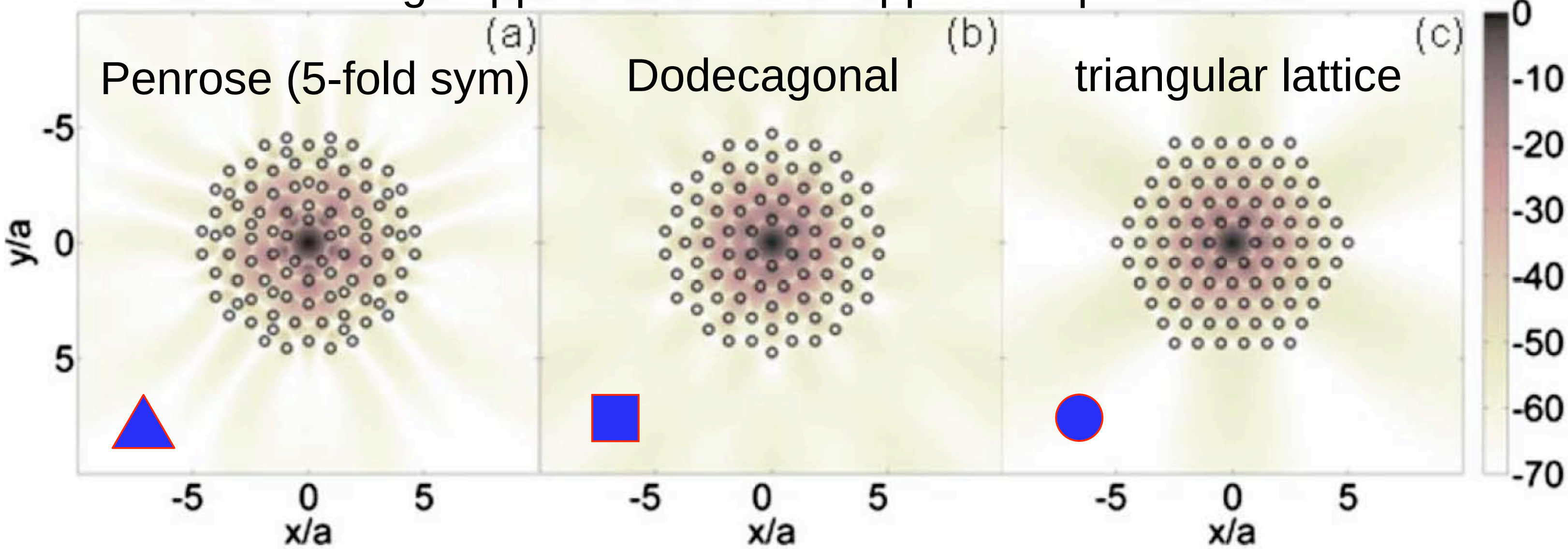

Measured and simulated frequencies agree within 2%.

Measured (open symbols) and simulated (closed) Q, near 17 GHz:

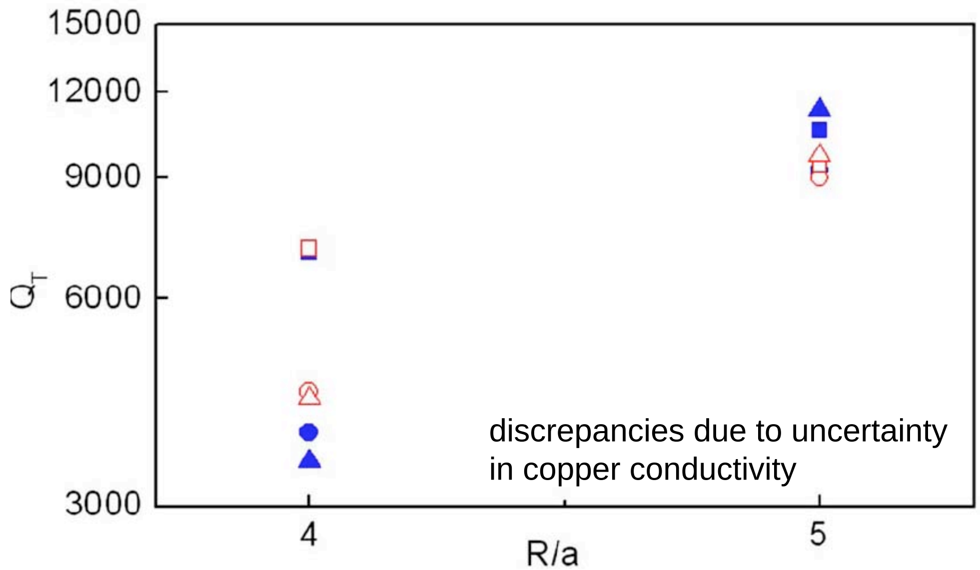

Simulations performed with CST Microwave Studio.

See E. Di Gennaro et. al., Appl. Phys. Letters 93, 164102 (2008).

Optimization of a PhC structure

to minimize radiation leakage (Q factor excludes dielectric losses)

36 alumina rods, Q = 500

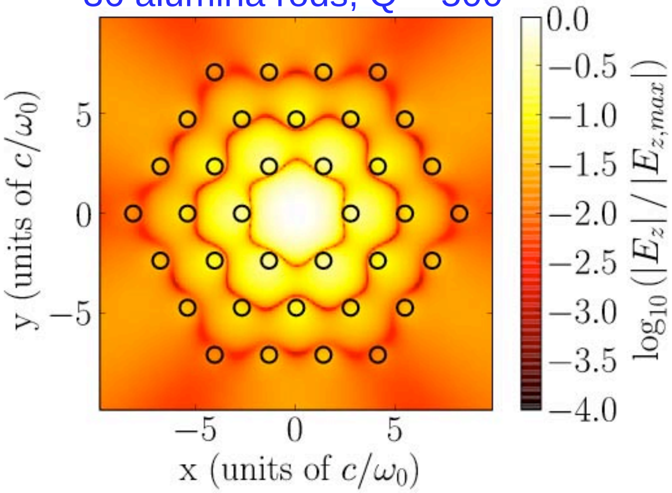

18 alumina rods, Q = 11,000

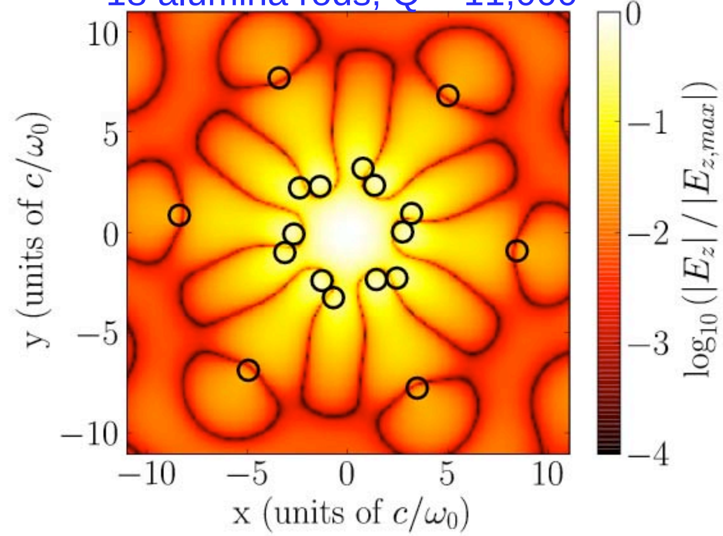

18 sapphire rods, Q = 25,000

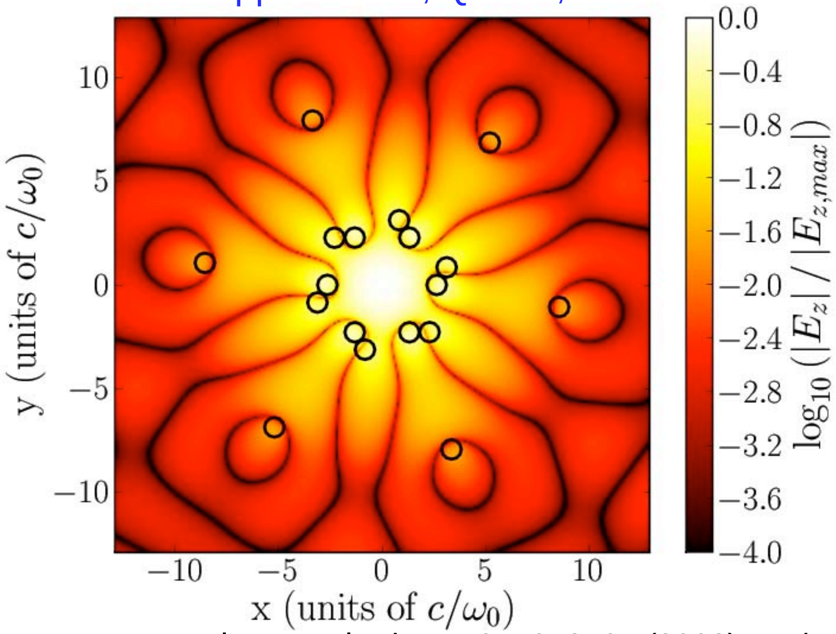

24 sapphire rods, Q = 190,000

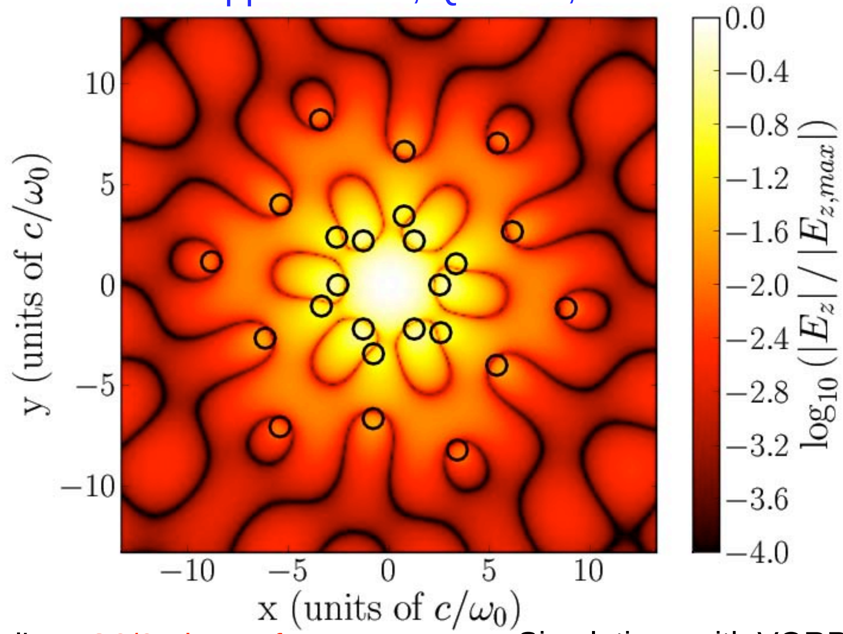

See C. A. Bauer et. al., J. Appl. Phys. 104, 053107 (2008), and AAC talk: WG2/3 Thurs afternoon

Simulations with VORPAL

Wakefields in optimized PhC cavities.

Metal Pillbox Cavity
(for comparison)

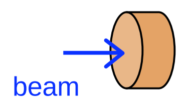

PhC Cavity

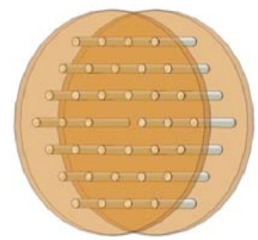

With 36 alumina rods, Q_{rad}=500

Optimized Cavity

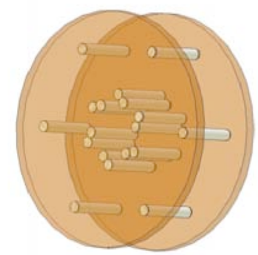

With 18 alumina rods, Q_{rad}=11,000

Accelerating mode

power spectrum of m=0 (monopole) wake potential

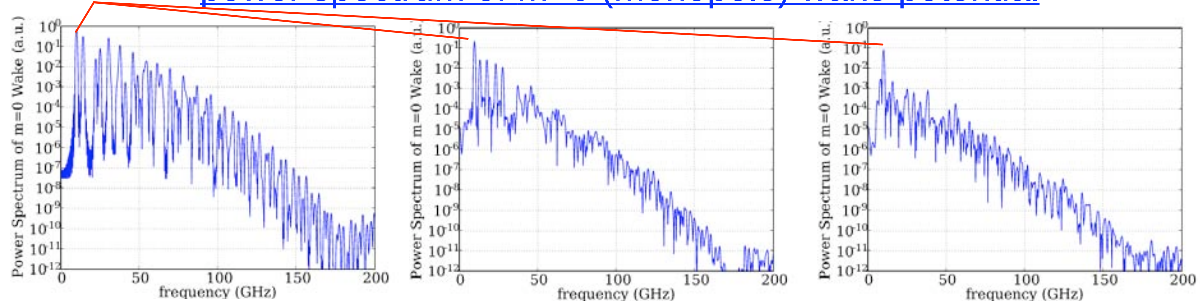

0.2-4 x 10^6 cells at 1 us/cell-step on 2 GHz Opteron circa 2003 with VORPAL.

power spectrum of m=1 (dipole) wake potential

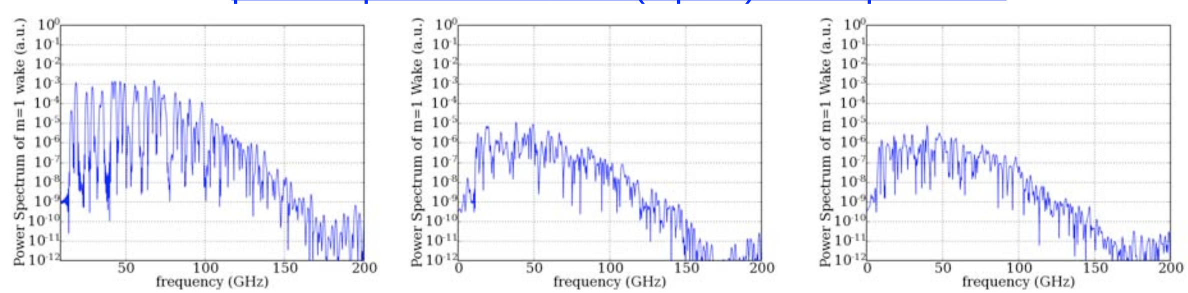

See G. R. Werner et. al., PRSTAB 12, 071301 (2009).

Wakefields were generated by a thin charge bunch offset from the axis by $0.14c/\omega_0$ and a Gaussian longitudinal distribution with $\sigma=0.25c/\omega_0$. The simulations were performed by VORPAL.

MIT metallic PhC cavity simulation vs. experiment

Axial electric field profile, simulation vs. measurement

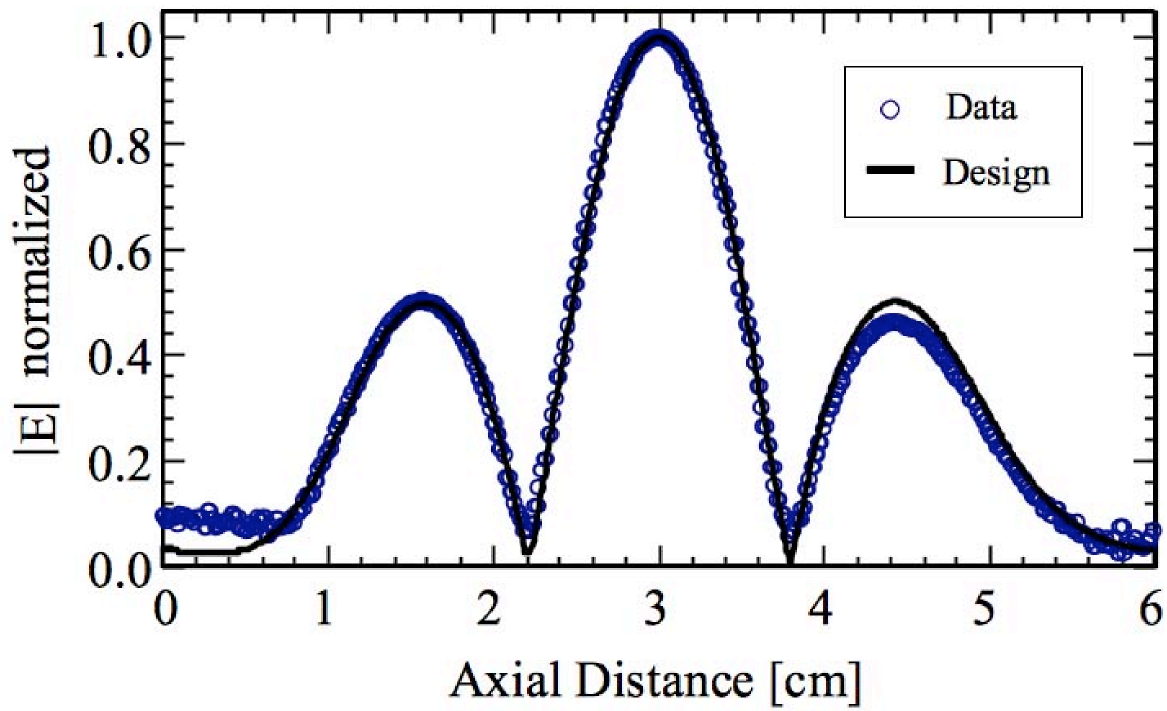

Eigensolve (or driven simulation) with HFSS: 700,000 tetrahedra,
12-24 hours computation time (on 8 cores).

See AAC talk by Brian Munroe: WG3 Tues morning
and R. Marsh's thesis: http://dspace.mit.edu.

MIT sapphire PhC cavity simulations

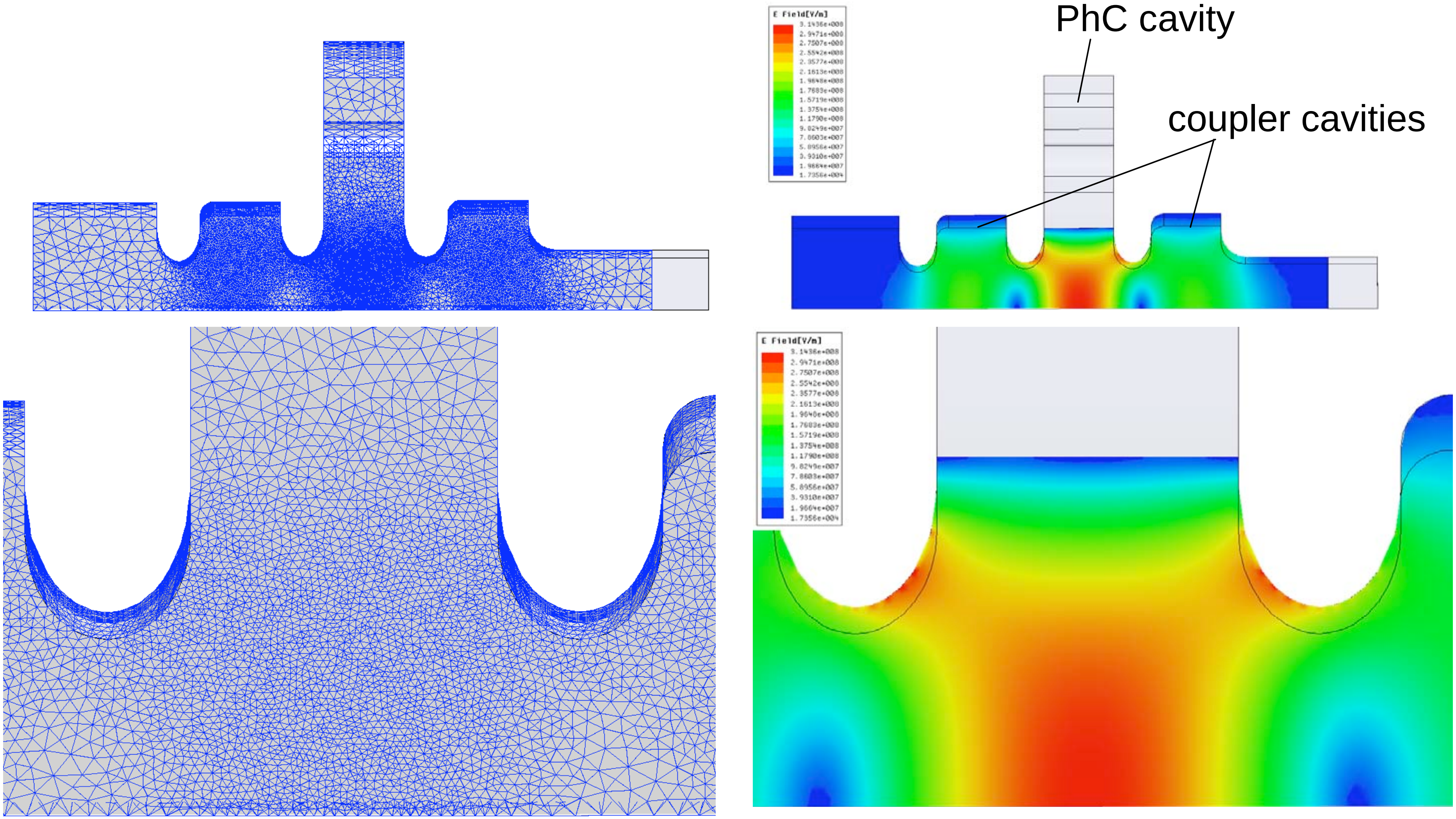

Simulations with HFSS: 670,000 tetrahedra in <100 core-hours on 2.7-3 GHz dual quad core Xeon.

See AAC talks Alan Cook: WG3 Fri morning
and R. Marsh’s thesis: http://dspace.mit.edu.

Overmoded cavity -- sapphire rods, Cu ends

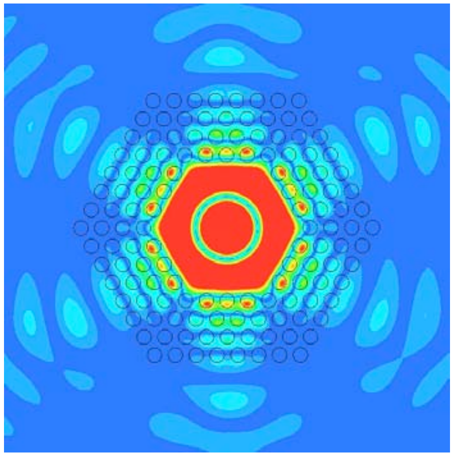

4 rows, $Q_{diff} \approx 500$

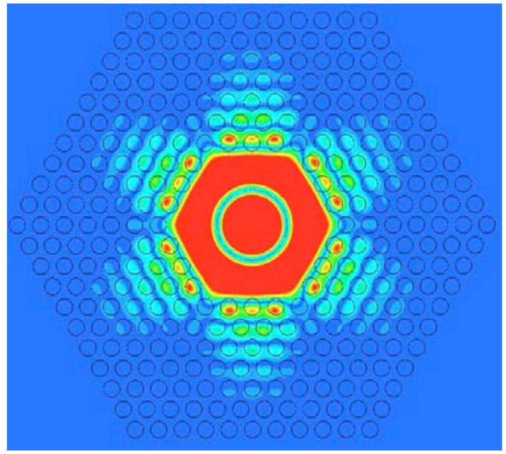

7 rows, $Q_{diff} \approx 19{,}000$

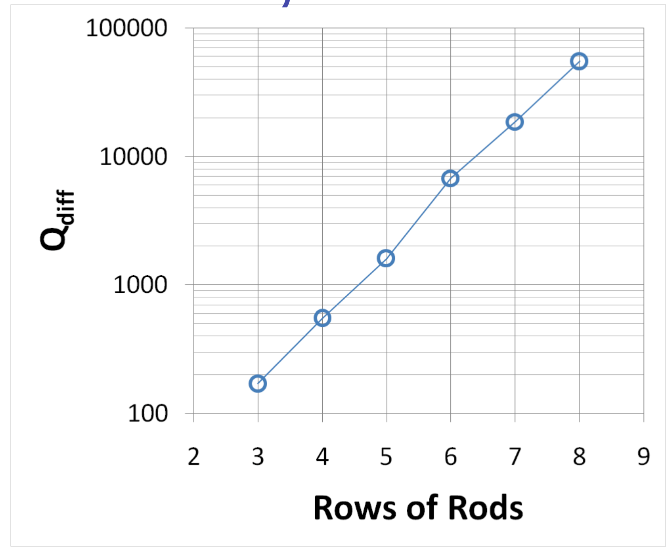

- HFSS simulation, PML boundary

Remove rods to create waveguides to carry away higher frequency modes:

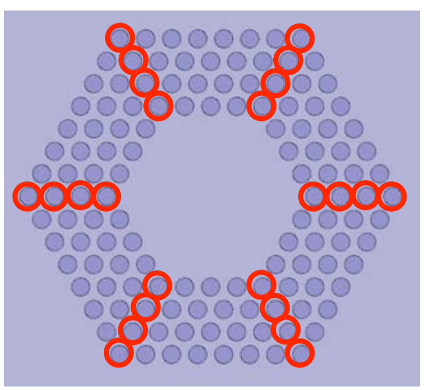

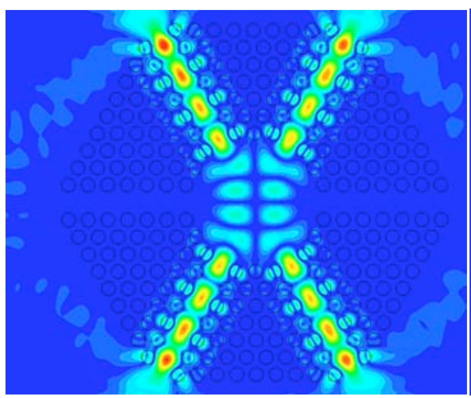

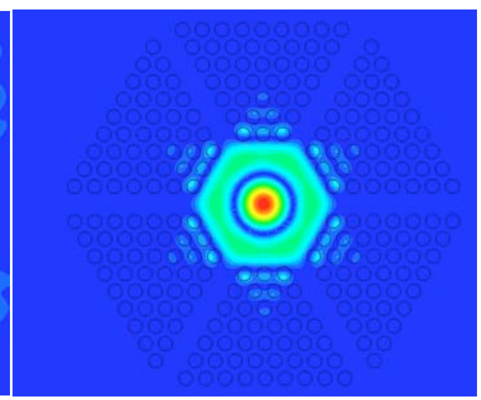

Mode	Diffrac. Q	Damped Q
TM_{02} 17 GHz	19,000	**18,000**
19 GHz	3500	**600**
31 GHz	$3*10^6$	**90**
31.1 GHz	$3*10^6$	**90**

Massachusetts Institute of Technology

See AAC talk by Alan Cook: WG3 Fri morning

Reducing pulse heating

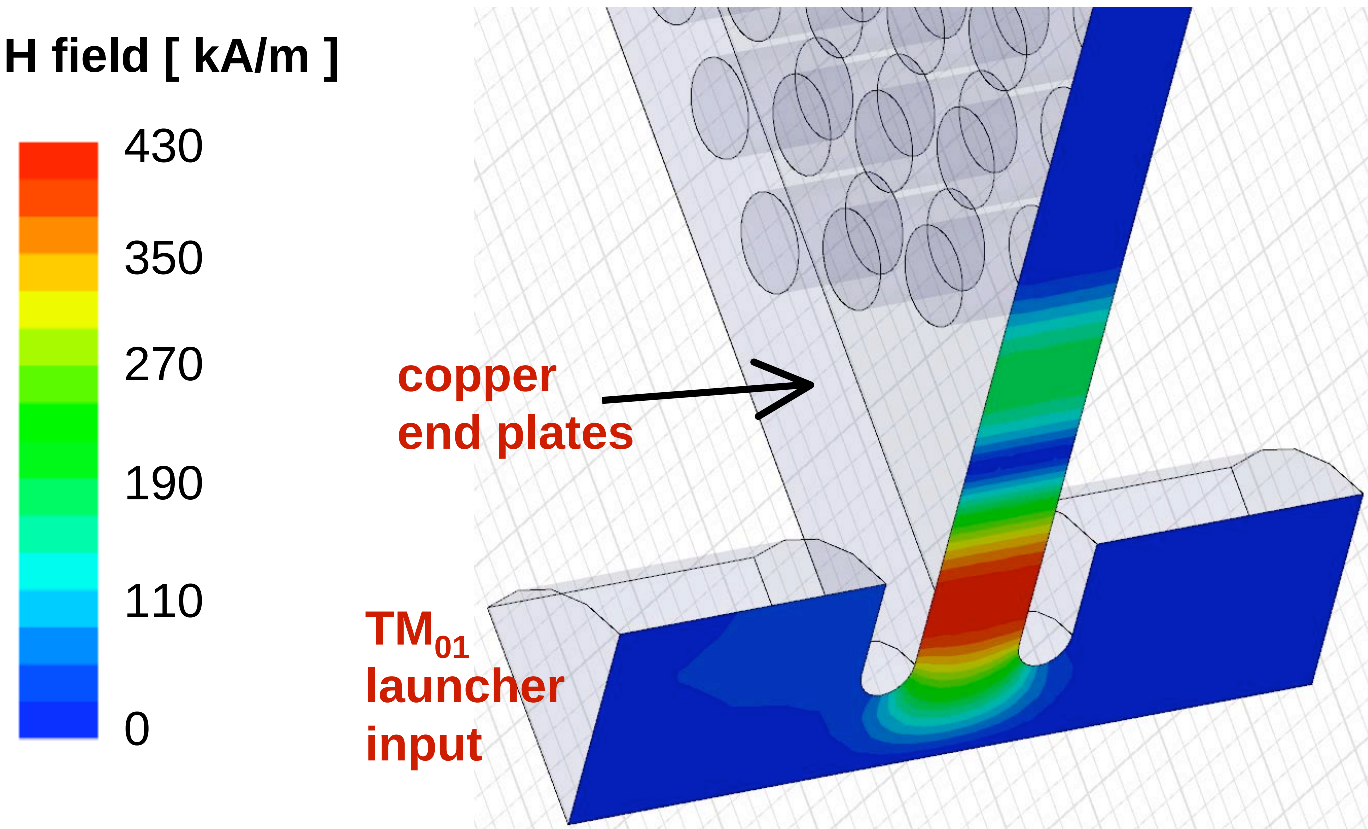

Simulated by HFSS

- Copper pulsed heating temp. rise: $\Delta T \approx$ 35K for 100 ns pulse, average accel. gradient $E_{acc} \approx$ 150 MV/m, 10 MW input power
- Below acceptable $\Delta T \approx$ 50K level

Massachusetts Institute of Technology

See Alan Cook's AAC talk: WG3 Fri morning
(also Brian Munroe's talk: WG3 Tues morning)

Woodpile Structure

a self-supporting 3D photonic crystal

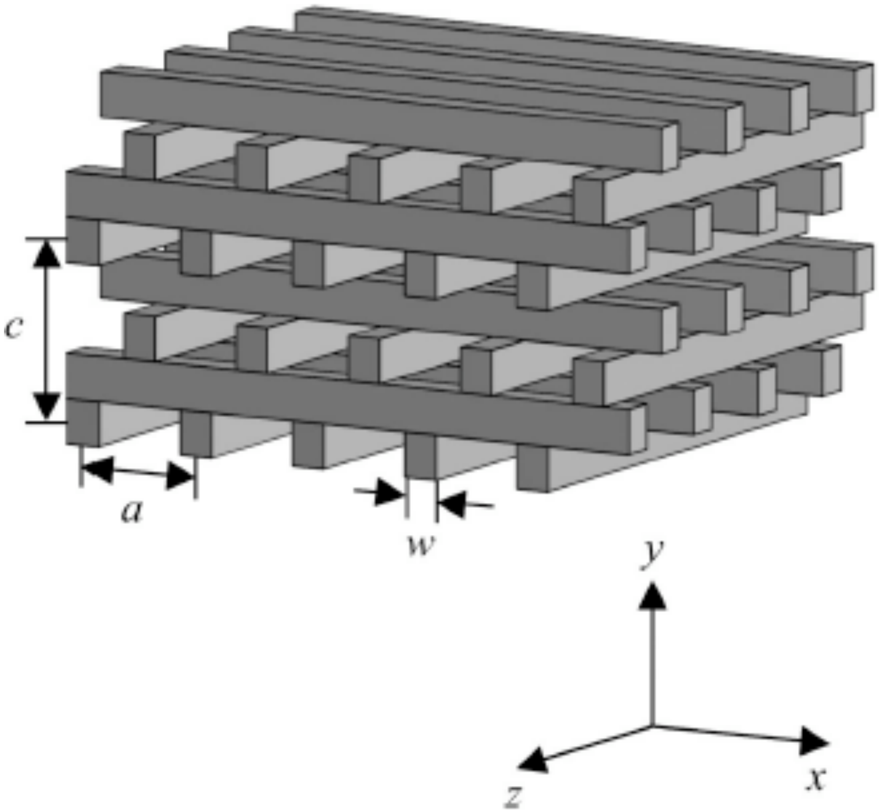

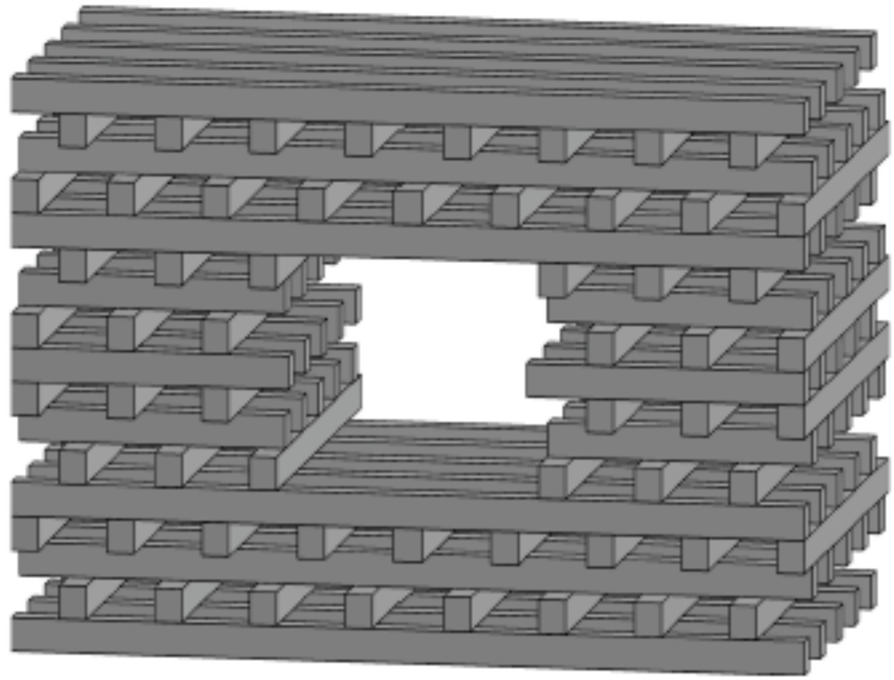

FIG. 3. A symmetric waveguide.

See B. M. Cowan, PRSTAB 11, 011301 (2008).

Woodpile structure for optical frequencies

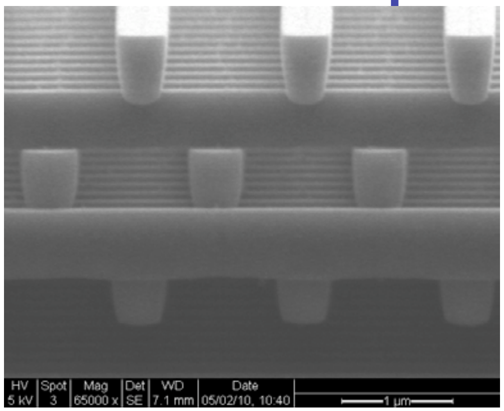

Simulation vs. Measurement: reflection from a woodpile structure with band gap.

Simulated with in-house RCWA code by A. Serpry (rigorous coupled-wave analysis, assumes infinite repetition of 2D planes)

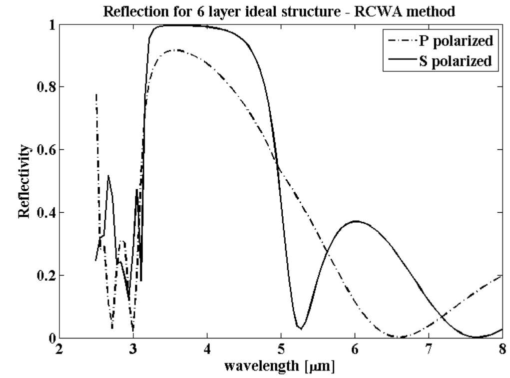

4 layers

6 layers

See C. McGuinness, E. Colby, and R. L. Byer, J. Mod. Opt. 56, 2142 (2009).

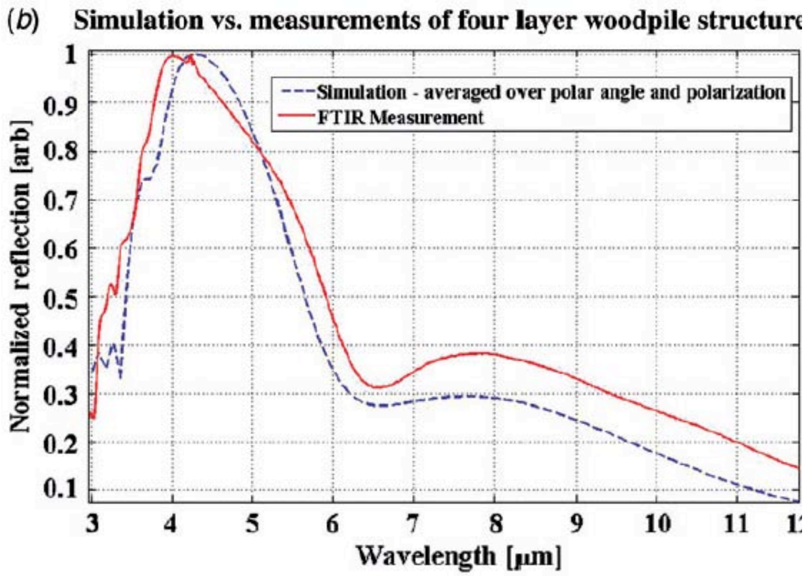

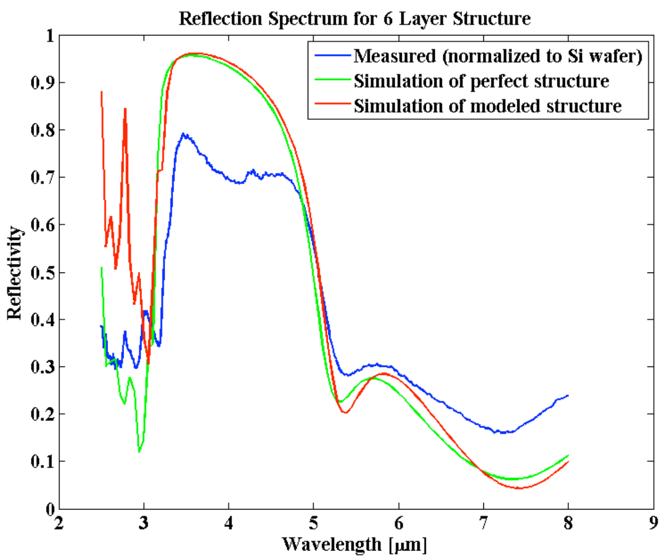

Here, units don't allow comparison of absolute reflection amplitude, but dependence on wavelength and band gap position show good agreement.

Band gap center discrepancy: 1%
Band gap FWHM discrepancy: 18%

Discrepancy in absolute amplitude at least partially due to uncertainty in Si reflectivity (used for normalization).

See AAC talk by Chris McGuinness: WG3 Fri afternoon

Woodpile with elliptical logs for Direct Laser Write lithography

Longitudinal Modes (Accelerating Modes)

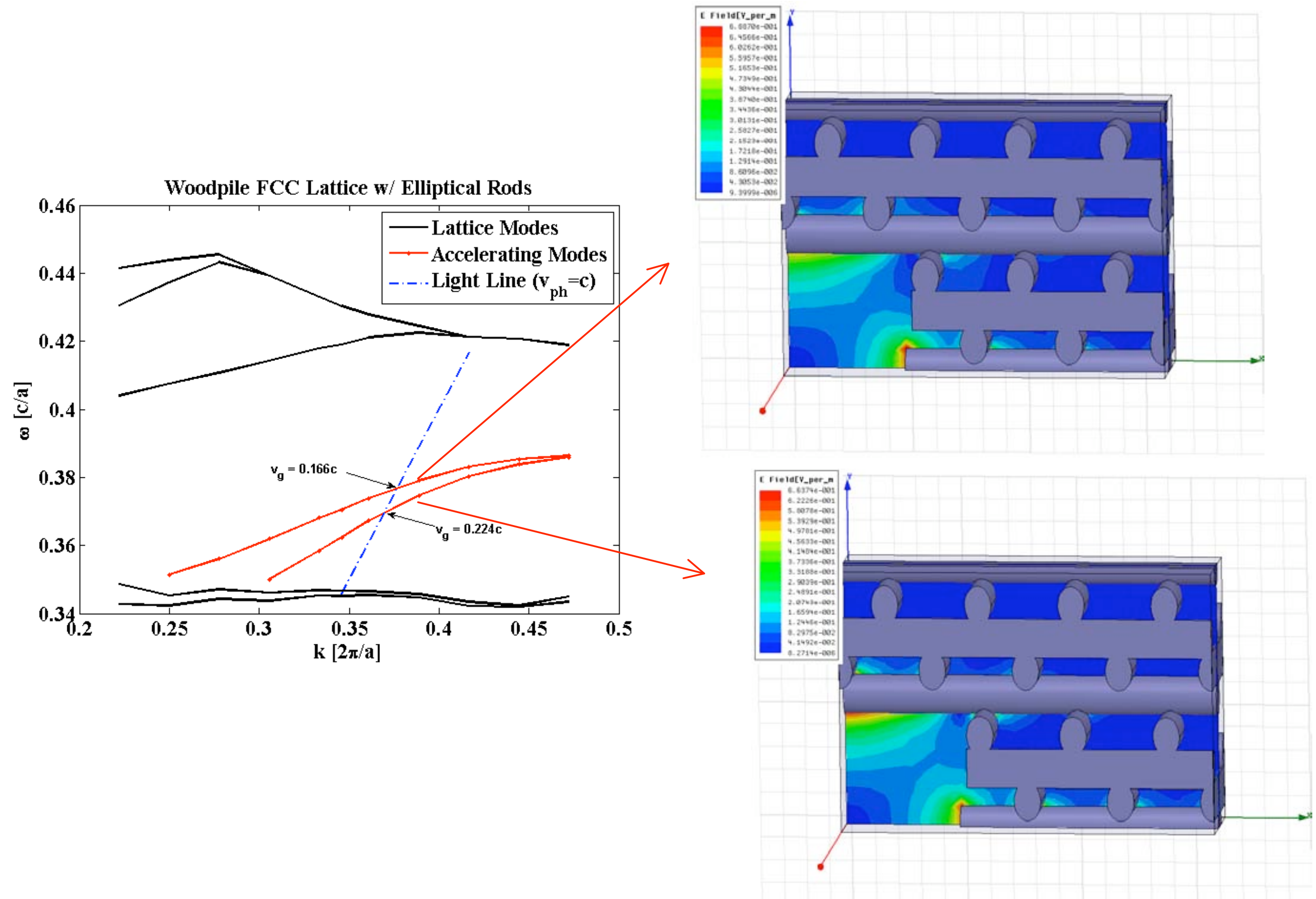

Simulations performed with HFSS.

See AAC10 talk by Chris McGuinness (WG3 Fri afternoon).

Optimizing Coupler for Woodpile Structure

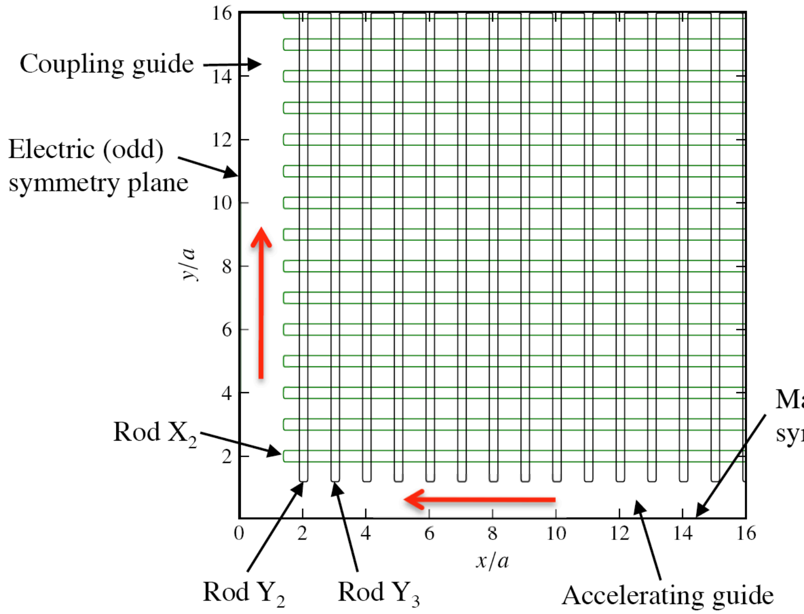

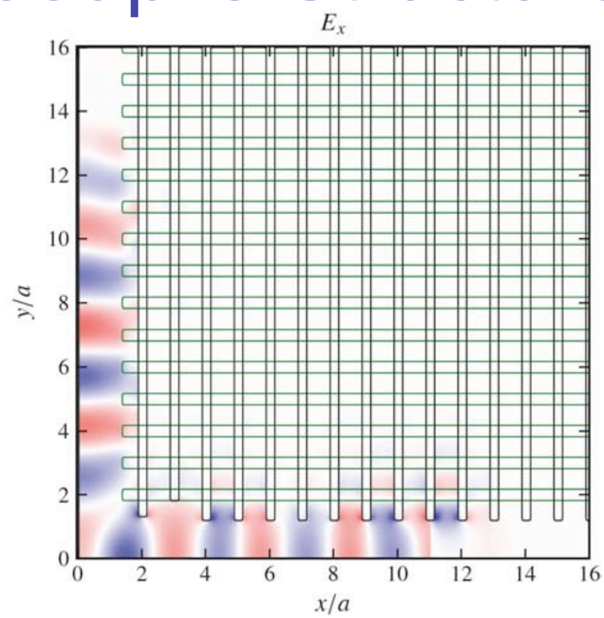

Optimized with VORPAL on 256 cores, 16 cells per lattice constant.

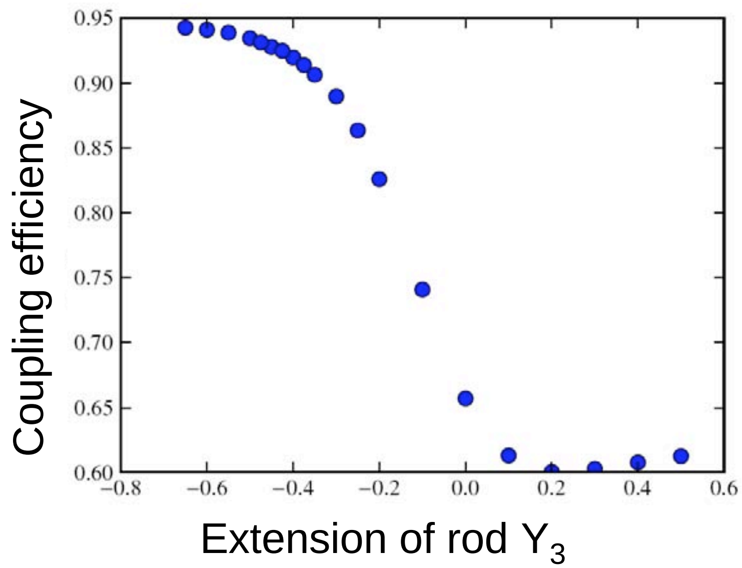

See B. M. Cowan et. al., IPAC 2010, THPEC013, and AAC talk Fri afternoon.

More complicated dielectrics

Nonlinear dielectrics: ε depends on electric field

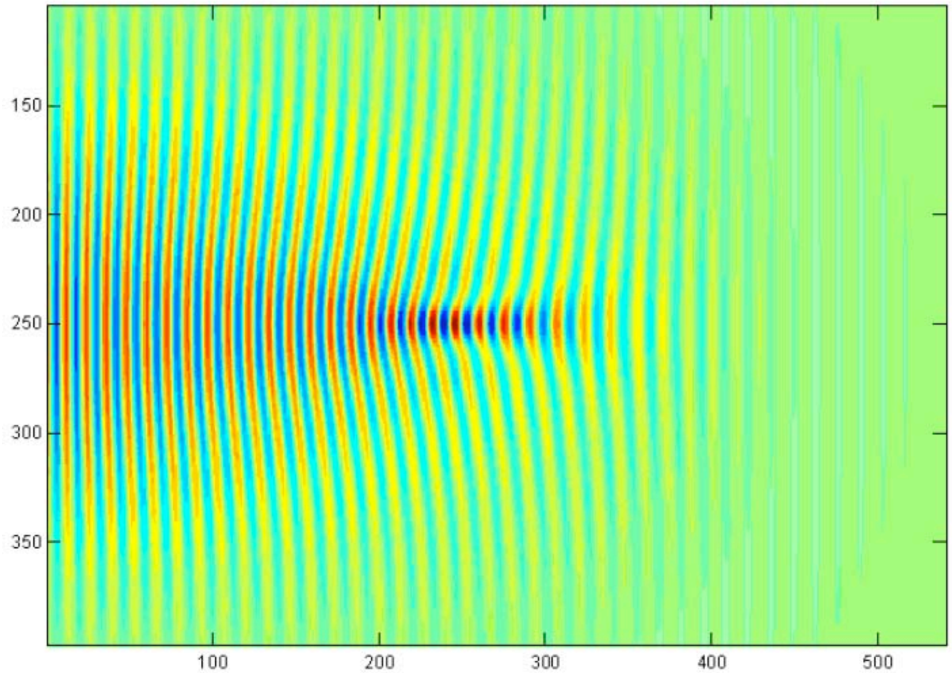

Figure 2. Kerr medium; Self focusing (H_z component of the field is plotted).

Also dispersive dielectrics: ε depends on frequency

See P. Schoessow, IPAC 2010 THPD070 and THPD069 and AAC presentations in WG6 Monday morning.

Metamaterial-loaded waveguide

Wires and split rings

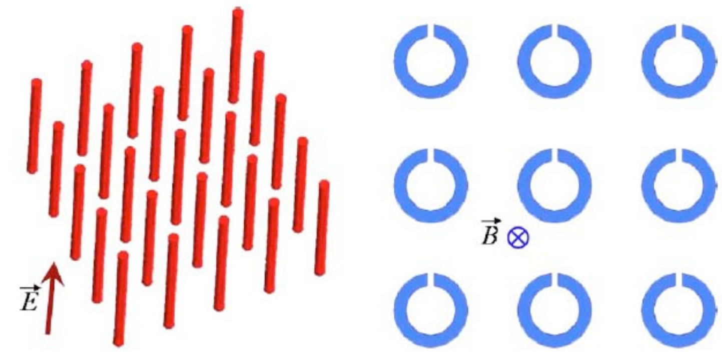

$$\varepsilon(\omega) = 1 - \frac{\omega_p^2}{\omega^2 + i\gamma\omega}, \quad \omega_p^2 = \frac{2\pi c^2}{a^2 \ln(a/r)}$$

$$\text{and } \gamma_e = \frac{c^2}{2\sigma S \ln(a/r)}.$$

$$\mu_{\text{eff}} = 1 - \frac{F\omega^2}{\omega^2 - \omega_{\text{res}}^2 + i\gamma\omega}.$$

yield double negative material

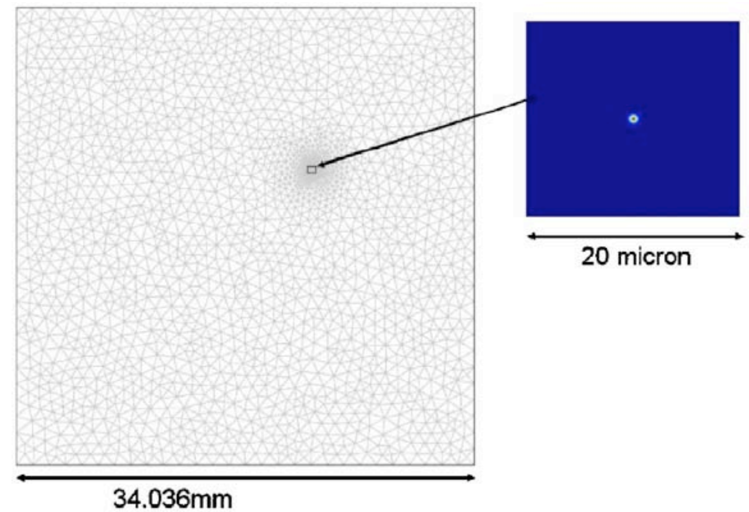

FIG. 9. (Color online) Irregular mesh in finite element method. Mesh is refined in the center to resolve a micron size off-centered beam with 1 nC charge passing through the waveguide.

In-house FEM 2D code used.

Misaligned beam excites more modes:

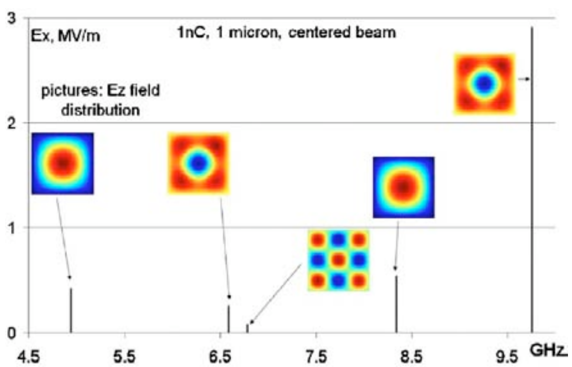

FIG. 11. (Color online) Beam passing through the center of the waveguide. E_x, MV/m on the sidewall of the waveguide spectrum. Pictures show the field distribution at particular frequency ω. Dipole modes are not excited because of symmetry.

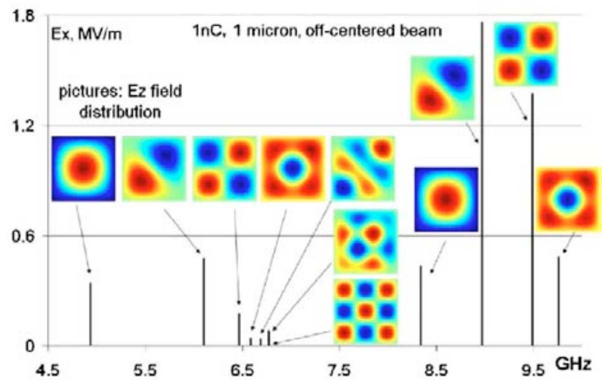

FIG. 10. (Color online) E_x, MV/m on the sidewall of the waveguide, spectrum. Pictures show the field distribution at particular value of a parameter ω.

See S. Antipov et. al., J. Appl. Phys. 102, 034906 (2007).

GPUs for faster computing?

VORPAL reports times for basic explicit FDTD update of 0.005 us/cell-step (for double precision; single precision is twice as fast) using GPU, a speed-up of approximately 20-40x. Not yet ready for commercial use. (See P. Messmer et. al., PAC 2009, FR5PFP084.)

Estimate for a basic update with dielectric: 0.006-0.007 us/cell-step for double precision.

This performance is parallelizable, but because of interprocessor communication costs, domain sizes have to be increased (if GPU is 50x faster, domains have to be 50x larger so simulation isn't dominated by communication). Domain size is limited by GPU memory (but 4 GB is a sizeable domain; and essentially this is no different from the domain size being limited by CPU memory).

CST Microwave Studio (see www.cst.com/Content/Products/MWS/GPU.aspx):

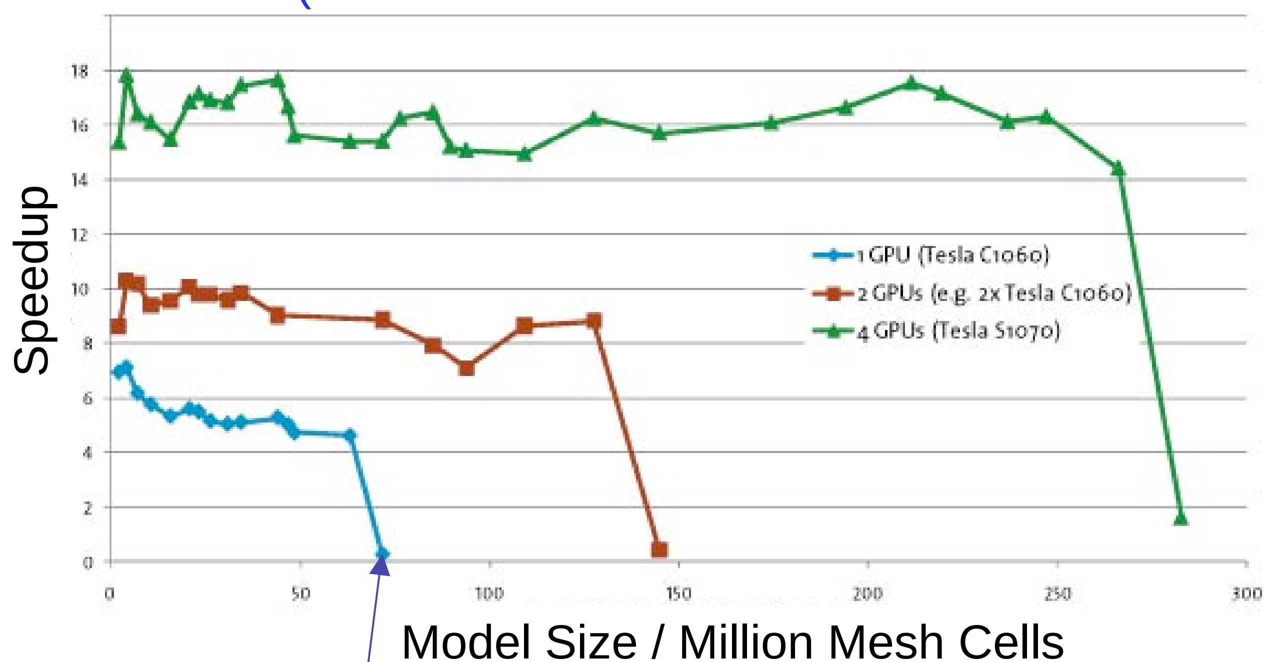

N.B. Size of double precision E-field vector for 75 million mesh cells: 1.8 GB; the GPU with 4 GB can barely hold two vectors.

GPUs for faster computing?

Recent work relevant to dielectrics: Crank-Nicolson (implicit) FDTD scheme for modeling (small) real 3D problems (S coefficients of microstrip elements) with dielectric, metal, and Mur absorbing boundary conditions.

With CPU (3 GHz Core 2): 80-90 us/cell-step
With same CPU and GPU (240 cores): 8-9 us/cell-step

on meshes of 10^5 cells using dt = 10 dt_CFL.

GPU offers a factor of 10 speed-up!

Ironically, for the demonstrated problems, a typical explicit FDTD algorithm on a CPU requires 0.1-0.2 us/cell-step, and would be 4-5 times faster than above (while obeying the Courant condition, dt = dt_CFL).

See K. Xu et. al., Progress In Electromagnetics Research 102, 381 (2010).

Thanks again to the contributors:

Sergey Antipov
Carl Bauer
Alan Cook
Ben Cowan
Chunguang Jing
Chris McGuinness
Peter Messmer
Brian Munroe
Gennadij Sotnikov